INVESTIGATION ON TRANSIENT PERFORMANCE OF SUPERCONDUCTING GENERATOR WITH GOVERNOR CONTROL AND STABILIZER

Thesis submitted in partial fulfilment of the requirements for the award of

degree of

Master of Engineering

in

Power Systems & Electric Drives

Thapar University, Patiala

By:

Devashish Sharma

(Regn. No. 80741007)

Under the supervision of

Dr. Sanjay K. Jain

Assistant Professor, EIED

JULY 2009

ELECTRICAL & INSTRUMENTATION ENGINEERING DEPARTMENT

THAPAR UNIVERSITY

PATIALA-147004

CERTIFICATE

I hereby certify that the work which is being presented in the thesis entitled, **"Investigation on transient performance of superconducting generator with governor control and stabilizer"**, in partial fulfilment of the requirement for the award of Master of Engineering in ***Power Systems & Electric Drives*** submitted in Electrical & Instrumentation Engineering Department of Thapar University, Patiala, is an authentic record of my own work carried out under the supervision of **Dr. Sanjay K. Jain**, Assistant Professor, EIED.

The matter presented in this thesis has not been submitted for the award of any other degree of this or any other university.

Devashish Sharma 15/07/09

(Devashish Sharma)
Regn. No. 80741007

This is to certify that the above statement made by the candidate is correct and true to the best of my knowledge.

Sanjay 15th July '09

(Dr. Sanjay K. Jain)
Assistant Professor
Electrical & Instrumentation Engg. Department
Thapar Univeristy
Patiala.

Countersigned by

S. Ghosh 15/7/09

(Dr. Smarajit Ghosh)
Professor & Head
Electrical & Instrumentation Engg. Department
Thapar University,
Patiala.

R K Sharma 16/7

(Dr. R.K.Sharma)
Dean(Academic Affairs)
Thapar University,
Patiala.

ACKNOWLEDGEMENT

On the completion of this thesis work, it is my proud privilege to express my deep sense of gratitude towards my thesis supervisor **Dr. Sanjay K. Jain, Assistant Professor**, **EIED** for his invaluable guidance, constant encouragement, suggestions, great patience, and continuous technical support which helped me, survive through crest and troughs of my thesis work and completed successfully. It is a great privilege to work under him, who motivated me in every course of my work and made me believe in myself.

It is a great pleasure to to express my special thanks to **Dr. Smarajit Ghosh**, **Professor and Head of Deptt.**, for his innovative suggestions and encouragement which helped me in completing this thesis work successfully. I also thank to **Dr. Yaduvir Singh, P.G. Coordinator** and all faculty members of EIED for their encouragement.

Much appreciations is expressed to **Prof. Abhijit Mukherjee, Director, Thapar University, Prof. K.K. Raina, Deputy Director, Thapar University** and **Prof. R.K. Sharma, Dean of Academic Affairs** to provide me moral support to go ahead with my innovative M.E. Thesis work.

I would like to thank my frieds, Mr. Sahil Gupta, Mr. Naveen Sethi, Mr. Javed Dhillon, Miss. Saranjeet Kaur and Mr. Ashutosh K. Tiwari for their encouragement and their affection. I would also like to thank one and all of my M.E. classmates for giving me constant encouragement, inspiration and suggestions.

I am very happy to express salutations to my parents because, my success, my failure, indeed every thing I own, belongs to them. I would also like to express my deep affection and best wishes to my loving sister Miss. Anamika Sharma for always being there to listen to me.

Devashish Sharma

80741007

ABSTRACT

Superconductivity is a phenomenon occurring in certain materials generally at very low temperatures, characterized by exactly zero electrical resistance and the exclusion of the interior magnetic field. The superconducting materials are gaining acceptance for large power applications like generator. Moreover, the superconducting generator possesses low inertia, low damping and therefore requires adequate control and stabilizer.

In this thesis work, a systematic approach to investigate the performance of synchronous superconducting generator is presented. The d-q model of the synchronous superconducting generator is developed in the synchronous reference frame for analysis. The performance characteristics of the superconducting generator with exciter, turbine and power system stabilizer are investigated with the help of extreme transients like grid connection, short circuit fault and opening of conductors. The performance of the superconducting generator is compared with conventional generator.

TABLE OF CONTENTS

LIST OF FIGURES

CHAPTER 1

INTRODUCTION

1.1 OVERVIEW

Energy has played a key role in human life since the Industrial Revolution that began in 1860s. The electrical energy has become the major form of energy for end use consumption in today's world. The benefit of the conversion is that electric energy is easy to transmit for long distance and flexible to distribute for customer's needs.

Superconducting generator have three potential benefits over conventional types. Without an iron core, they can operate at higher magnetic fields (up to 5-6 T) and thus have 50% less size and weight. This translates into reduces material requirements, capital cost, and manufacture-induced impact on the environment. Second, superconducting generators offer greater system stability against frequency and load variations in the grid. Their smaller size leads to smaller synchronous reactance, thereby enhancing the critical clearing time after a fault condition. Finally, due to their higher efficiency and thus fewer emission per generated kWh.

With respect to the electric power industry, the superconducting ac generator has the greatest potential for large-scale commercial application of superconductivity. Such a machine should be able to convert mechanical energy to electric energy more efficiently and with greater economy of weight and volume than any other method. These advantages can be accrued at a scale of 1200 MVA output, with the added potential of operation at transmission line voltage, and greater system stability.

The most important aspects in the performance of the superconducting alternators are those affecting their transient operation. The superconducting machine is characterised by its low p.u. reactance, high hunting frequency and low inherent damping. The latter two characteristics are expected to produce some adverse effects on transient performance, however the low reactance tends to increase stability limits.

The typical structure of the system is shown in Fig. 1.1. The system considered is a superconducting generator (SCG) connected to an infinite bus power system. The SCG

has superconducting field windings in the rotor, surrounded by two separate screens. The inner screen, which has a relatively long time constant, shields the superconducting field windings from external, time varying magnetic fields. The outer screen serves as a damper and has a substantially shorter time constant than that of the inner screen.

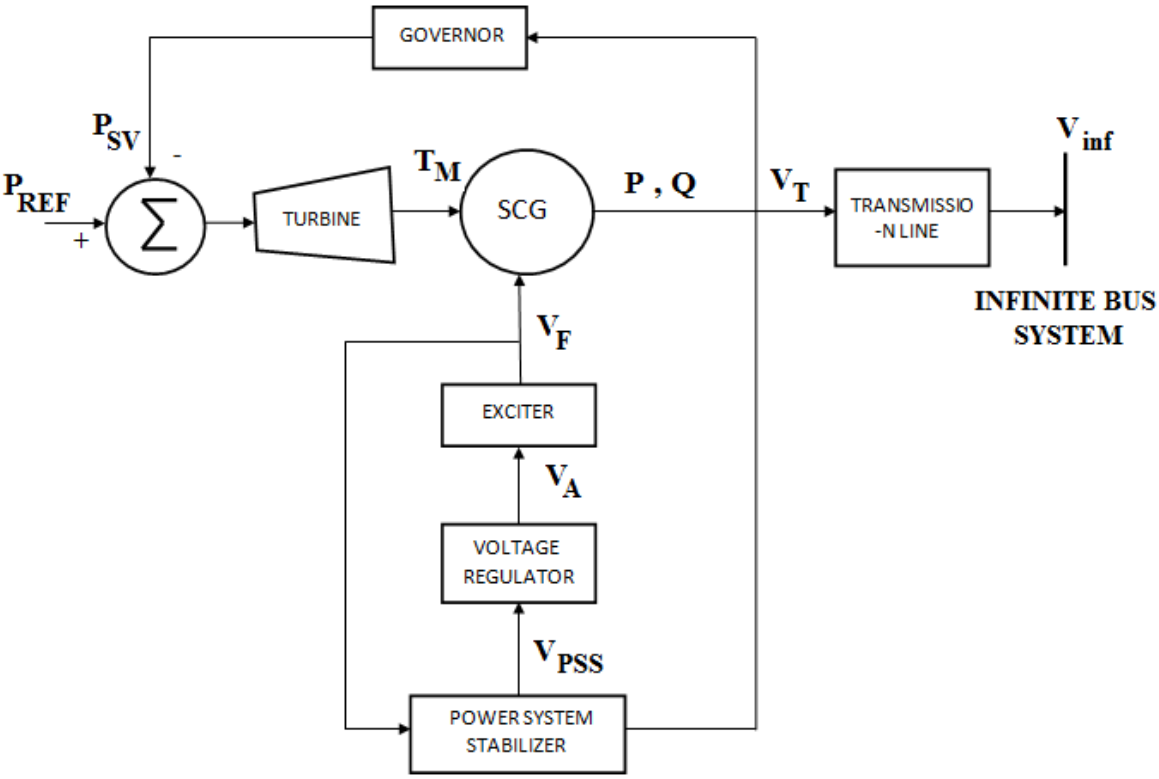

Figure 1.1: Single machine infinite bus system

The excitation control system is an automatic feedback control having the primary function of maintaining a predetermined terminal voltage by modifying the field current of the synchronous generator based on changes in the terminal voltage. The exciter is the device that provides the field current for the synchronous generator. The automatic voltage regulator (AVR) couples the terminal voltage to the input of the main exciter.

Power system stabilizer (PSS) controller design, methods of combining the PSS with the excitation controller (AVR), and investigation of many different input signals and the vast field of tuning methodologies. The action of a PSS is to extend the angular stability limits of a power system by providing supplemental damping to the oscillation of

synchronous machine rotors through the generator excitation. This damping is provided by a electric torque applied to the rotor that is in phase with the speed variation. The turbine-governor control helps in controlling the rotor oscillations and damping. The steady state power output can be changed by turbine control.

1.2 LITERATURE REVIEW

The concepts incorporating superconducting technology in electrical machine have been proposed soon after the construction of the first successful superconducting magnets in 1961. During the mid sixties some work on ac superconducting machines was started in the United States primarily under military contracts.

The earliest work on superconducting generators was done in the U. S. in 1964 -1966 in which an alternator was successfully demonstrated by Sykulski and Goddard [1] using a fixed superconducting field coil, and a rotating normal armature with slip ring connections. Within a few years, studies on similar superconducting synchronous machines have being conducted around the world.

In 1973 Kirtley and Edeskuty [2], have summarized the feasibility and potentials for the application of superconductors in the rotating field windings of large central station. In 1977, two competing superconducting generator programs at Westinghouse and General Electric were successfully completed with the objective to develop a 1200 MVA unit of superconducting generator.

In 1997, Japan has build and tested three 70 MW superconducting ac generators using NbTi (niobium-titanium) low temperature superconductor cooled by liquid helium. The rotors have been design for high stability, high critical current density, and low ac losses. Demello and Concordia [3] have proposed the affect of excitation control for the improvement of stability of synchronous machine.

Godhwani, Kim and Eberly [4] have designed the digital excitation system. Design and testing feature of digital excitation control has been highlighted. Kirtley [5] described large system interaction characteristics of superconducting generator. The difference between superconducting generators and conventional machines has been highlighted in

1994, General Electric started to design a 100 MVA high temperature superconducting generator.

Ueda and Shiobara [6] have proposed the measurement and analysis of 70MW superconducting generator constants. The comparison between the test results and the values calculated by three dimensional finite element methods is summarized. Ahmed and Bashar [7] has discussed the use of superconducting magnetic energy storage devices in a power system. He has also discussed the efficiency improvement method by using a superconducting storage coil with gas turbine power. The prime mover runs a synchronous generator, with the output rectified to feed a dc bus. The additional of a superconducting magnetic energy storage coil can improve overall system performance.

Saleh and Bolton [8], have designs fuzzy logic stabilizer for a superconducting generator with help of genetic algorithm. The important aspect of the design of superconducting generators concerns stability following a major system disturbance has been presented. Because the superconducting field winding has a very long time constant, turbine governor control is crucial for improving transient and dynamic stability. Ying-Yi and Wen-Ching [9] have proposed new approach optimization for tuning parameters of power system stabilizers. A novel approach using optimization, a root coefficient relationship and basic control theory of stabilizer for generator has been summarized.

Kundur and Klein [10] have proposed papers on application of power system stabilizers for enhancement of overall system stability and gives detailed account of analytical work carried out to determine the parameters of power system stabilizers for a large generating station. Lubosny and Bialek [11] have discussed the power system stabilizer design for small synchronous generator and gives study analysis of static excitation control with automatic voltage regulator.

Dai and Shokooh [12] has discussed the generator start up study of hydro turbine unit for a generation facility with improvement method of efficiency and stability control system. Alyan and Rahim [13] have proposed the role of governor control in transient stability of superconducting turbogenerator. They have discussed the effect of mechanical power control on transient stability of superconducting alternator. Minseok [14] has discussed

the dynamic performance and design of a high critical temperature of superconducting synchronous generator.

Michael [15] has presents papers on high temperature superconductor field windings for homopolar generator with exciter and power system stabilizer in simulation analysis. He also discussed the environmental impacts of superconducting power applications. The idea about environmental advantages that superconducting devices could bring to power system networks have been discussed, superconducting electrical machine even more preferable from environmental point of view.

1.3 OBJECTIVE OF THE WORK

The work reported in the thesis has been carried out with the objective to investigate the transient performance analysis on superconducting generator and to study the effect of various controls resulted by turbine-governor and power system stabilizer on its performance during various transient conditions like grid connection and faults.

1.4 ORGANIZATION OF THESIS

The work presented in this thesis is organized in six chapters. These six chapters are structured as follows.

Chapter 1 This chapter is entitled as **"Introduction"**. The overview, the literature review, aim and organization of thesis are discussed briefly.

Chapter 2 This chapter is entitled as **"Superconducting Materials".** The review on superconductivity and superconducting material, their relative features and application area are summarized. The various design aspect of superconducting generator in comparison to conventional generator is also presented.

Chapter 3 This chapter is entitled as **"Mathematical Modelling of the System".** It introduces a mathematical model of synchronous generator, turbine, exciter and power system stabilizer.

Chapter 4 This chapter is entitled as **"Digital Simulation of System using SIMULINK".** This chapter details the methodology to simulate the system in SIMULINK and in MATLAB environment.

Chapter 5 This chapter is entitled as **“Results and Discussion”**. This chapter is focused on the results pertaining to the performance of system under various conditions.

Chapter 6 This chapter is entitled as **"Conclusions and Future work"**, this chapter summarized the conclusions drawn for the study and the scope for future work.

CHAPTER 2

SUPERCONDUCTIVITY AND SUPERCONDUCTING MATERIAL

2.1 INTRODUCTION

Superconductivity is the property of some materials in which electrical resistance is zero, and they acquire the ability to carry electric current with no loss of energy. An electric current flowing in a loop of superconducting wire can persist indefinitely with no power source.

Traditional superconductors operate at absolute zero temperature (-459.67^0 Fahrenheit (F) or -273.15^0 Celsius). Experiments in the 1980s raised the temperature to -321^0 F. By the late 1990s, superconductivity was demonstrated at -164^0 F. The superconductors are used to make alloys of niobium, for high-powered magnets in medical imaging machines and particle accelerators. Superconducting materials have low power dissipation, high-speed operation, and high sensitivity [16]. They also have the ability to prevent external magnetic fields from penetrating their interiors and are perfect diamagnetism. Superconductors have applications in medical imaging, magnetic energy-storage systems, motors, generators, transformers, computer components, and sensitive magnetic-field measuring devices. Superconductivity occurs in a wide variety of materials, including simple elements like tin and aluminium, various metallic alloys and some heavily-doped semiconductors.

In 1986 the discovery of a family of cuprate-perovskite ceramic materials known as high-temperature superconductors, with critical temperatures in excess of 90^0 kelvins (K), spurred renewed interest and research in superconductivity for several reasons. These materials represented a new phenomenon not explained by the current theory. In addition, because the superconducting state persists up to more manageable temperatures, past the economically-important boiling point of liquid nitrogen (77^0 K), more commercial applications are feasible, especially if materials with even higher critical temperatures could be discovered. In addition to temperature, a material's ability to superconductivity depends heavily on two other variables. Superconductors operate in magnetic fields, but

there is a field strength beyond which superconductivity is lost. This is known as the critical magnetic field. The maximum current that a superconductor can carry is called the critical current. If any of these "critical" factors temperature, magnetic field strength, or amount of current is exceeded, superconductivity is destroyed. The challenge is to design systems and devices that can operate under the "ceiling" set by these three variables

2.2 THE HISTORY OF SUPERCONDUCTORS

Superconductivity was discovered in 1911 by Heike Kamerlingh Onnes, who was studying the resistance of solid mercury using liquid helium as a refrigerant. As shown in Fig. 2.1, at the temperature of 4.2 K, the resistance abruptly disappeared. The temperature at which a material becomes superconducting is known as the transition, or critical, temperature (Tc), and it varies for different materials. In subsequent decades, superconductivity was found in several other materials under certain temperature and pressure [17]. In 1913, lead was found to superconduct at 7 K, and in 1941 niobium nitride was found to superconduct at 16 K.

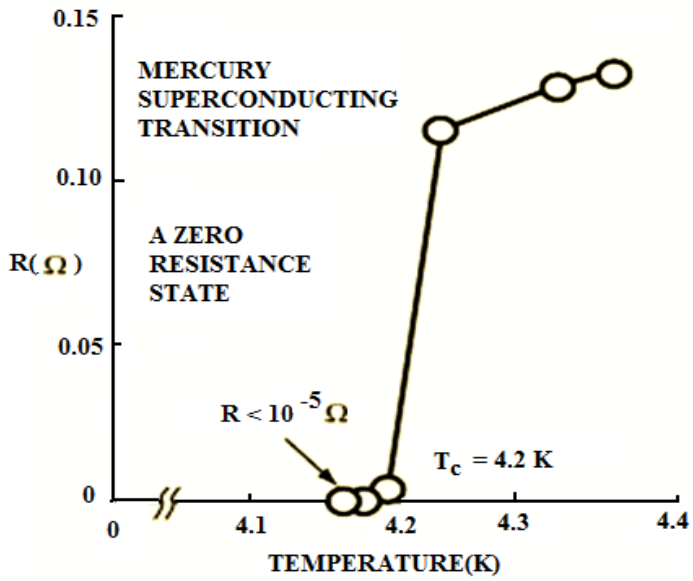

Figure 2.1: A zero resistance state of superconducting materials

The next important step in understanding superconductivity occurred in 1933, when Meissner and Ochsenfeld discovered that superconductors expelled applied magnetic fields, a phenomenon which has come to be known as the Meissner effect. In 1935, F. and H. London showed that the Meissner effect was a consequence of the minimization of the electromagnetic free energy carried by superconducting current.

In 1950, the phenomenological Ginzburg-Landau theory of superconductivity was devised by Landau and Ginzburg. This theory, which combined Landau's theory of second-order phase transitions with a Schrödinger-like wave equation, had great success in explaining the macroscopic properties of superconductors. In particular, Abrikosov showed that Ginzburg-Landau theory predicts the division of superconductors into the two categories now referred to as Type I and Type II.

The complete microscopic theory of superconductivity was finally proposed in 1957 by Bardeen, Cooper, and Schrieffer and is regarded as BCS theory. This BCS theory explained the superconducting current as a superfluid of Cooper pairs, pairs of electrons interacting through the exchange of phonons.

In 1962, the first commercial superconducting wire, a niobium-titanium alloy, was developed by researchers at Westinghouse, allowing the construction of the first practical superconducting magnets. In the same year, Josephson made the important theoretical prediction that a supercurrent can flow between two pieces of superconductor separated by a thin layer of insulator. This phenomenon, now called the Josephson effect, is exploited by superconducting devices such as SQUIDs.

In 2008 it was discovered by Valerii Vinokur and Tatyana Baturina that the same mechanism that produces superconductivity could produce a super insulator state in some materials, with almost infinite electrical resistance.

2.3 SUPERCONDUCTING PROPERTIES

Most of the physical properties of superconductors vary from material to material, such as the heat capacity and the critical temperature, critical field, and critical current density

at which superconductivity is destroyed. On the other hand, there is a class of properties that are independent of the underlying material. For instance, all superconductors have exactly zero resistivity to low applied currents when there is no magnetic field present. The existence of these "universal" properties implies that superconductivity is a thermodynamic phase. Various properties of superconducting materials include-

- Energy Gap.
- Zero Resistance.
- Superconducting Electromagnets.
- High temperature superconductors.

These properties are explained in brief:

- **ENERGY GAP**

Most thermodynamic properties of superconductors are found to vary as $e^{-\Delta/kBT}$ with temperature indicating the existence of a gap or energy interval with no allowed Eigen energies in the energy spectrum. In the elementary properties of superconductors the most of the physical properties of superconductors vary from material to material, such as the heat capacity and the critical temperature, critical field, and critical current density at which superconductivity is destroyed.

- **ZERO RESISTANCE**

All superconductors have exactly zero resistivity to low applied currents when there is no magnetic field present. The existence of these "universal" properties implies that superconductivity is a thermodynamic phase, and thus possess certain distinguishing properties which are largely independent of microscopic details. The resistance of the sample is given by Ohm's law. If the voltage across the sample made of superconducting material is zero when current is passed, this means that the resistance is zero and that the sample is in the superconducting state.

- **SUPERCONDUCTING ELECTROMAGNETS**

Superconductors are also able to maintain a current with no applied voltage whatsoever, a property exploited in superconducting electromagnets such as those found in magnetic resonance imaging (MRI) machines. Experiments have demonstrated that currents in superconducting coils can persist for years without any measurable degradation.

- **HIGH TEMPERATURE SUPERCONDUCTORS**

In superconducting materials, the characteristics of superconductivity appear when the temperature T is lowered below a critical temperature T_c. The value of this critical temperature varies from material to material. Conventional superconductors usually have critical temperatures ranging from around 20 K (kelvins) to less than 1 K. Solid mercury, for example, has a critical temperature of 4.2 K. The highest critical temperature found for a conventional superconductor is 39 K for magnesium diboride (MgB_2), this material has a doubt about classifying it as a "conventional" superconductor. Cuprate superconductors can have much higher critical temperatures: $YBa_2Cu_3O_7$, one of the first cuprate superconductors to be discovered, has a critical temperature of 92 K, and mercury-based cuprites have been found with critical temperatures in excess of 130 K. The explanation for these high critical temperatures remains unknown. Electron pairing due to phonon exchanges explains superconductivity in conventional superconductors, but it does not explain superconductivity in the newer superconductors that have a very high critical temperature.

2.4 TYPES OF SUPERCONDUCTORS

Superconductors are classified into two types

- Type-1 superconductors.
- Type-2 superconductors.

2.4.1 TYPE-1 SUPERCONDUCTOR

The Type 1 category of superconductors is mainly comprised of metals and metalloids that show some conductivity at room temperature. They require incredible cold to slow down molecular vibrations sufficiently to facilitate unimpeded electron flow in accordance to BCS theory. BCS theory suggests that electrons team up in "Cooper pairs" in order to help each other overcome molecular obstacles - much like race cars on a track drafting each other in order to go faster.

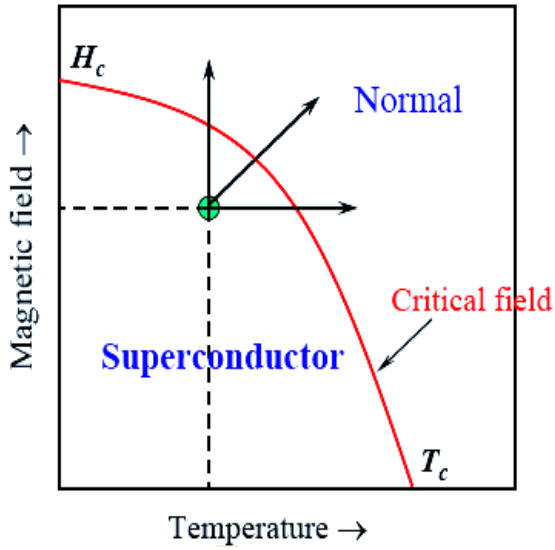

Figure 2.2: Type 1 superconductor

Type 1 superconductors - characterized as the "soft" superconductors - were discovered first and require the coldest temperatures to become superconductive. They exhibit a very sharp transition to a superconducting state and "perfect" diamagnetism - the ability to repel a magnetic field completely as shown above in Fig. 2.2. Many additional elements can be coaxed into a superconductive state with the application of high pressure [18]. For example, phosphorus appears to be the Type 1 element with the highest Tc. But, it requires compression pressures of 2.5 Mbar to reach a Tc of 14-22 K.

2.4.2 TYPE- II SUPERCONDUCTOR

All high-temperature superconductors are Type II and these elements exhibits the “mixed” magnetic state. Except for the elements vanadium, technetium and niobium, the Type 2 category of superconductors is comprised of metallic compounds and alloys. The recently-discovered superconducting "perovskites" (metal-oxide ceramics that normally have a ratio of 2 metal atoms to every 3 oxygen atoms) belong to this Type 2 group. They achieve higher Tc's than Type 1 superconductors by a mechanism that is still not completely understood. Conventional wisdom holds that it relates to the planar layering within the crystalline structure. Fig. 2.3 shows the properties of type -II superconductors.

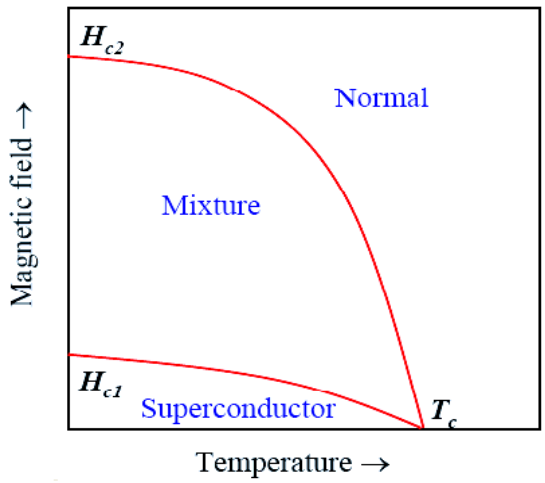

Figure 2.3: Type -II superconductors

Type 2 superconductors - also known as the "hard" superconductors - differ from Type 1 in that their transition from a normal to a superconducting state is gradual across a region of "mixed state" behaviour.

2.5 ADVANTAGES AND LIMITATIONS OF SUPERCONDUCTORS

Superconductors have several pronounced advantages compared to conventional conductors which are explained below

- Superconducting material can carry much higher currents, create vastly larger magnetic fields, and carry electric current with no energy loss to resistance.
- Superconducting materials can transmit much larger amounts of electricity than conventional wires of the same size.
- These type of material now used in various electric power applications, such as motors, generators, transmission cables, and transformers.
- Superconducting motors, transformers, and other applications using high temperature superconducting wire will be half the size of conventional machines with the same power rating, and have half the energy losses. This will be enormously beneficial to the way electricity is generated, delivered, and used.

There are the following limitations of superconductors

- Superconductors are very sensitivity to high currents as well as to magnetism. At high currents, superconductors can cease functioning properly, and magnetic fields are particularly deadly to superconductors, easily reverting them back to normal conductors.
- Unfortunately, the superconductors developed to date can only exist in a super-cold environment, far below room temperature. This requirement makes them impractical to use in many situations and very difficult to study. In addition, the materials that currently lend themselves to becoming superconductors don't as yet have the flexibility that makes electrical wire so convenient. Often the materials developed are available only in very tiny quantities.

2.6 ELECTRIC POWER APPLICATIONS

A variety of electric power applications for superconducting wire are proposed or now in development. The electric power devices and components being designed to incorporate superconducting technology will operate more efficiently and less expensively than their conventional alternatives. The potential of superconducting technology is inspiring: power plants could generate electricity using less fuel and producing fewer emissions; electric motors could be smaller and much more powerful; power cables could transmit

3–5 times more electricity; and energy could be stored much more efficiently. Superconductivity has been in the marketplace for more than 20 years, in equipment such as MRIs, magnetic separators, magnets, and high-energy physics devices such as particle accelerators and in particle detectors used by astronomers. These applications are described below

- **MAGNETIC RESONANCE IMAGING (MRI)**

The core of an MRI machine is a powerful magnet. MRI systems built with HTS magnets could eventually be smaller and more powerful than is now possible with LTS-based systems. Further advances in MRI, made possible by HTS technology, would reduce costs, making medical imaging much more accessible. In 1993, U.S. manufacturers shipped roughly 400 MRI machines having a total value of $800 million. Unit prices range from $1 million to as high as $3 million, in sizes common in hospital and outpatient settings. Smaller, lower-cost units tend to dominate the market. If perfected, HTS technology could greatly expand this market.

- **TRANSMISSION CABLES**

Transmitting electricity is a natural fit for HTS technology. The dominant attraction of underground underground HTS cables is that they can carry three to five times more current than conventional copper cables [19]. Some HTS cable designs are based on retrofitting existing underground pipes that hold low-capacity conventional cables. In these systems, HTS wire is woven around a central pipe that carries liquid coolant. Multiple layers of thermal and electrical insulation protect the assembly. Old cable in many urban areas can be replaced with HTS cable, enabling increased power transmission through existing conduits. HTS cables may also be used in areas where overhead lines are rejected for environmental or aesthetic reasons.

- **MOTORS AND GENERATORS**

In conventional motors and generators, magnetic fields are generated by large coils of copper or aluminum wire. HTS wire can carry much larger electrical currents, which means remarkably smaller and more powerful systems. For instance, a 1,000 horsepower HTS motor can be 50% smaller than a conventional motor of the same power.

Manufacturing operations of all kinds could benefit from systems that take up less space and provide increased working capacity. In addition, substituting HTS wire for conventional wire eliminates energy loss due to electrical resistance, enabling motors and generators to operate with up to 98% and 99.5% efficiency, respectively. Today's typical generator operates at an efficiency rate of 97%–98%; a typical motor at 90%–96%.

- **TRANSFORMERS**

Transformers are relatively simple devices. Their sole purpose is lowering or raising system voltages in order to transport electricity more efficiently. Voltages are raised or lowered by inducing a new current (and voltage) in one coil by the magnetic field of a second coil. Electricity generally passes through at least three transformers before it is used by a consumer; three to six percent of all generated electricity is lost to transformer inefficiencies. In an HTS transformer, coils will be made from HTS wire instead of copper, reducing these losses by half. Additionally, HTS transformers will be as much as 50% smaller, and will no longer pose a fire hazard because they will not require flammable cooling oil. These are attractive benefits to utilities that have space limitations or want to increase their grid efficiency, as HTS-outfitted transformers can be placed closer to—even on top of or inside— buildings, relieving cramped substations.

- **MAGNETIC ENERGY STORAGE**

One shortcoming of the modern utility grid is its inflexibility; once manufactured, electricity must be used immediately. There is no pool of electricity available to accommodate momentary or long-term surges in demand. Accordingly, generators must be held on standby or started up for periods of excessive electricity demand, which is highly inefficient. New techniques based on superconductivity offer solutions to the problem. Energy storage depots can be created, which allow electricity to be deposited or withdrawn depending on circumstances. Utilities have recently identified distribution substations as valuable locations for these depots. Other customers have identified the need to protect sensitive equipment from momentary disturbances in power supply. Two approaches are currently being investigated: one based on flywheels and the other on magnetic fields. Flywheel energy storage devices rely on spinning discs that float on superconducting magnets and store energy in the motion of their rotation. Once charged,

these discs will spin almost indefinitely, without losing any of their energy to friction. Another storage technique, superconducting magnetic energy storage, relies on large superconducting coils to store energy as a powerful magnetic field. The major benefits of these systems is that they have energy efficiency rates in excess of 90%, as compared to batteries, which have limited lifetimes, and efficiency rates of only 80%–90%. If these superconducting techniques are perfected, the energy storage industry could be revolutionized.

2.7 SUPERCONDUCTING GENERATOR

Here the model of superconducting machine is shown in Fig. 2.4. The outermost element of the machine rotor also serves multiple purposes, the outer wall of the thermal isolation vacuum vessel and it is part of the rotor shielding and damping system, made of conductive material, it carries shielding currents that reduce time-varying fields in the region of the cryogenic shield and cold region. It also serves as a damper, similar to the amortisseur of conventional machines [5].

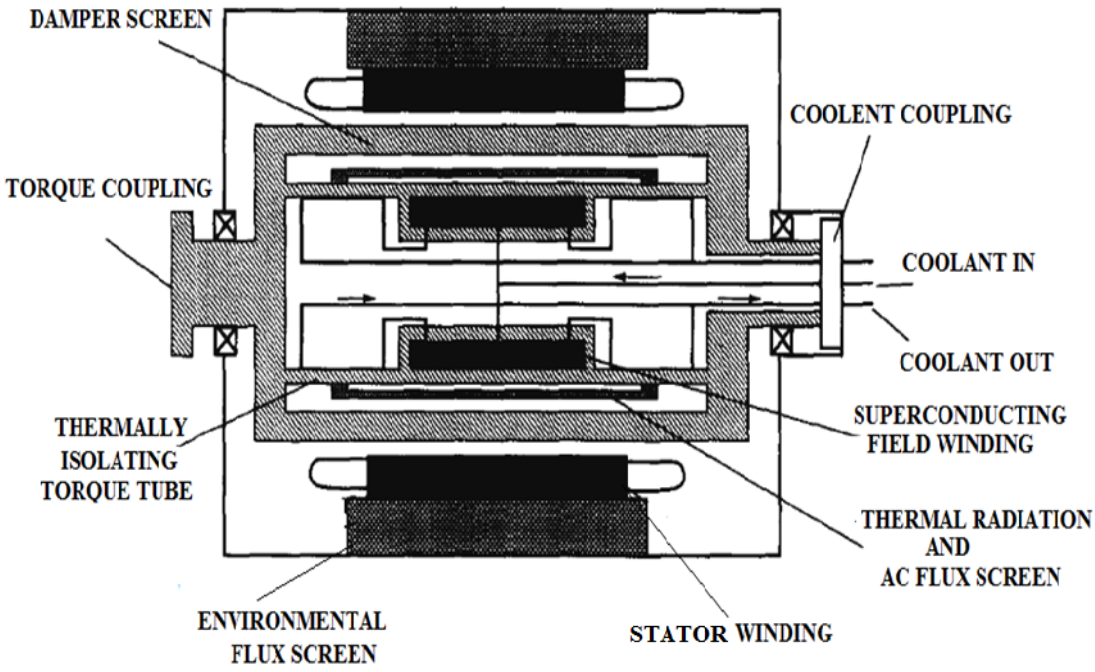

Figure 2.4: Superconducting machine

The coolant stream is coupled to the rotor at one end through a relative rotation coupling. Cryogenic fluid is transferred to the rotor and gaseous effluent is transferred back out. Superconducting generators have stator windings of the “air-gap’’ type. Conventional, bar-in-slot armatures would have the same power limitation as conventional machines: flux linkage determined by tooth saturation and current determined by cooling through the bars. Air-gap armatures can carry more current because they have higher space factors and are not limited in flux density by iron teeth. This type of armature depends on the high MMF of the superconducting field winding. The “stator core” in a conventional machine is laminated iron stationary part of the magnetic circuit, which becomes as an “environmental screen” in the superconducting generator, since it does little to increase the magnetic interaction field but is, required confining the large rotating dipoles. Unique operating characteristics of superconducting generators are due to the enormous current densities achievable by superconducting field windings. Such field windings can produce magnetic flux densities in excess of saturation levels in iron, but with no iron. Thus superconducting machines are air-core and consequently have very low reactance’s. They also have high power density, which when coupled with the absence of iron from the rotor, means low inertia. The near-zero resistance of the field winding and the need for good shielding of the cold rotor from time-varying magnetic fields lead to long rotor electrical time constants.

CHAPTER 3

MATHEMATICAL MODELLING OF THE SYSTEM

3. 1 GENERAL

A generator is an electromechanical machine composed of a static part (the stator) and a rotating part (the rotor) whose relative position is changed periodically by rotating angle ωt. In general, synchronous machines can be catalogued into two types according to air gaps between stator and rotor:

- Synchronous machine with uniform air gaps and concentric cylindrical rotor, such as surface mount permanent machine
- Synchronous machine with non uniform air gaps, such as salient pole of machine, interior permanent machine (IPM), etc.

Excitation system performs control and protective functions for generator. The direct current required for field excitation is furnished by the excitation system. The source of power can be a shaft-mounted exciter, a motor-generator set, or a static rectifier. Turbine and governors is the prime mover for generator. They convert the primary energy of fuel into mechanical energy. Power system stabilizers are used to add damping to the generator power oscillations by controlling its excitation using an auxiliary stabilizing signal. To provide damping, the stabilizer must add a component of electrical torque in phase with rotor speed deviation.

3.1.1 REFERENCE FRAME THEORY

As is well known, the reference frame theory plays an important role to the analysis of different electric machines. All analysis presented here are based on the reference frame theory.

In the late 1920s, Park [20] proposed a new approach for electric machine analysis. He formulated a change of variables which replaced the variables (voltages, currents and flux linkages) associated with the stator windings of a synchronous machine with variables associated with windings rotating with the rotor. In other words, he transformed, or referred, the stator variables to a frame of reference in the rotor. Park's transformation,

which revolutionized electric machine analysis, has the unique property of eliminating all time-varying inductance from the voltage equations of the synchronous machine which occur due to:

- Electric circuits in relative motion
- Electric circuits with varying magnetic reluctance.

The model of a basic two pole salient pole synchronous superconducting machine with damper windings is shown in Fig. 3.1. The *d* axis is aligned with the N-pole of the rotor and *q* axis is 90 degree apart from *d* axis.

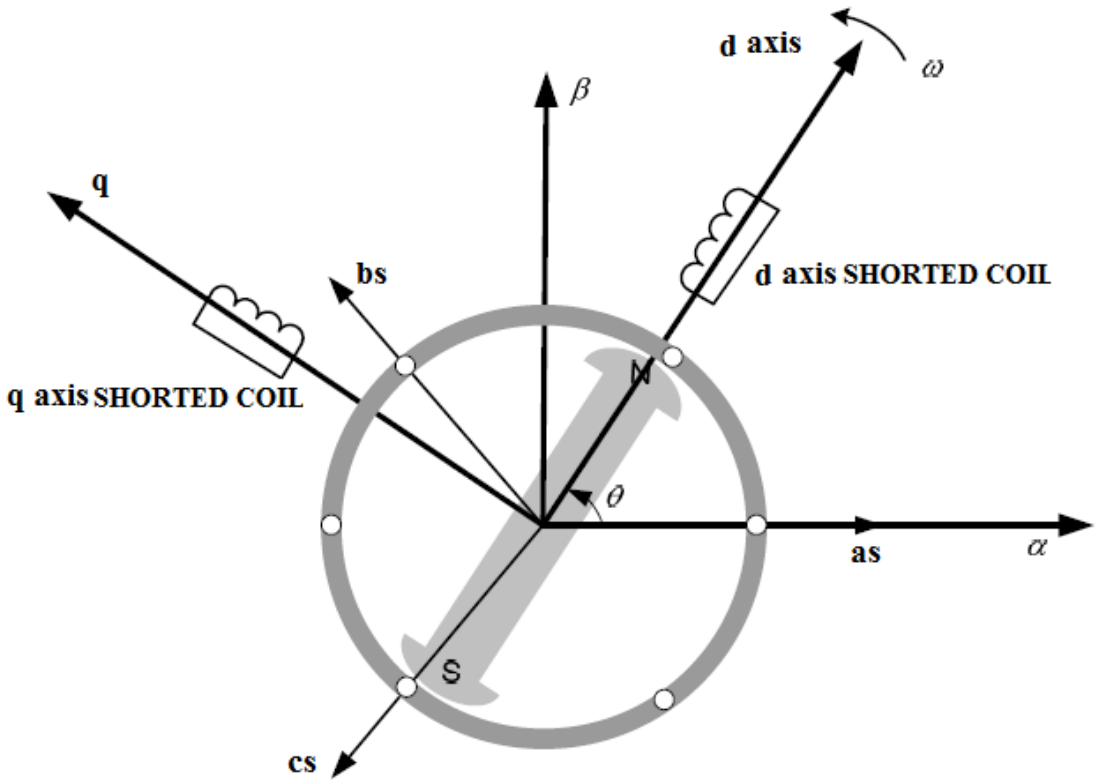

Figure 3.1: Model of a basic two pole salient pole synchronous superconducting machine

Two-pole machine is shown above; a multi-pole machine with any number of pairs of poles can be treated as a two-pole machine electrically, because armature (stator) windings are identically arranged with respect to each pair of poles.

As the rotor has two axes of mechanical rectangular symmetry, we call them the‘d-axis’ and ‘q-axis’. Namely:

- d-axis or direct-axis: the axis from the axial centre point in the pole direction.
- q-axis or quadrature-axis: the axis from the axial centre point in the direction 90^0ahead (leading) of the d-axis.

The field winding (named ‘d-axis filed coil’) is a closed circuit field windings connected to a source of d.c. voltage E_{fd}, and with an inductance to produce flux only in the direction of the d-axis.

The flux may flow into the left-hand side (i.e. the +q-axis component) and right-hand side (i.e. the -q-axis component) of the d-axis. Typical hydraulic-turbine-driven generators (vertical type with salient poles) have amortisseur or squirrel-cage windings in the pole face (damper windings), which consists of copper bars through the pole connected at their ends as a closed circuit. Thermal or nuclear-turbine-driven generators (horizontal type with cylindrical non-salient poles) have field windings only and do not have such damper windings. However, eddy currents are forced to flow into the pass of the rotor solid steel for the duration of transient or current-unbalanced conditions.

The stator has three stator windings in name for phases a, b and c connected at their ends commonly as the neutral terminal. The three windings are arranged electrically by 120^0 symmetrically to each other. This is justify from the assumption that the stator windings are sinusoidally distributed along with the air gap as far as all the mutual effects of the rotor are concerned, because the generator windings are distributed so as to minimize harmonics in its design.

3.1.2 RELATIVE ANGULAR POSITION BETWEEN ROTOR AND STATOR

The stator is immovable and the rotor is rotating counter clockwise at an angular speed of $\omega = \frac{d\theta}{dt}$ therefore the relative position between the rotor and the stator is measured by the rotating angle of the rotor d-axis. That is the rotating position of each coil in time can be written as follows on a d-axis basis:

Stator a phase coils : $\theta_a = \theta = \omega t = 2\pi f t$

b phase coil : $\theta_b = \theta + 240^o = \theta - 120^o = \omega t - 120^o$

	c phase coil	: $\theta_c = \theta + 120^o = \omega t + 120^o$
Rotor	field coil	: 0^o
	damper d-axis coil	: 0^o
	damper q-axis coil	: $+90^o$

3.2 GENERATOR MODEL

To handle the machine behaviour properly there is requirement of general (advanced) models. These advanced models for transients include the following

- Phase-variable model.
- d–q variable model.
- d-q model neglecting stator transients.

3.2.1 THE PHASE-VARIABLE MODEL

The phase-variable model of the synchronous superconducting generator is described by a set of three stator circuits coupled through motion with two (or a multiple of two) orthogonally placed (*d* and *q*) damper windings and a field winding (along axis *d*: of largest magnetic permeance, shown above in Figure 3.1. The stator and rotor circuits are magnetically coupled with each other. Synchronous superconducting machine is generally operated as a generator so that it is convenient to assume that the direction of positive stator current is out of the terminal [21]. With the convention the voltage equation in the machine variable may be expressed in matrix form as

$$v_{abc} = -r_s i_{abc} + p\lambda_{abcs} \quad (3.2.1)$$

$$v_{dqr} = -r_r i_{dqr} + p\lambda_{dqr} \quad (3.2.2)$$

Where

$$(f_{abcs})^T = [f_{as} \quad f_{bs} \quad f_{cs}] \quad (3.2.3)$$

$$(f_{dqr})^T = [f_{kq1} \quad f_{kq2} \quad f_{fd} \quad f_{kd}] \quad (3.2.4)$$

In the above equations the s and r subscripts denote variables associated with the stator and rotor windings, respectively. Both r_s and r_r are diagonal matrices

$$R_s = diag[r_s \quad r_s \quad r_s] \tag{3.2.5}$$

In the figure the positive as, bs and cs axes are drawn in the direction of negative flux linkage relative to the assumed positive direction of stator currents. In this case flux linkage equation become

$$\begin{bmatrix} \lambda_{abcs} \\ \lambda_{dqr} \end{bmatrix} = \begin{bmatrix} L_s & L_{sr} \\ (L_{sr})^T & L_r \end{bmatrix} \begin{bmatrix} -i_{abcs} \\ i_{dqr} \end{bmatrix} \tag{3.2.6}$$

Here Ls is as

$$L_s = \begin{bmatrix} L_{ls} + L_A - L_B cos2\theta_r & -\frac{1}{2}L_A - L_B cos2\left(\theta_r - \frac{\pi}{3}\right) & -\frac{1}{2}L_A - L_B cos2\left(\theta_r + \frac{\pi}{3}\right) \\ -\frac{1}{2}L_A - L_B cos2\left(\theta_r - \frac{\pi}{3}\right) & L_{ls} + L_A - L_B cos2\left(\theta_r - \frac{2\pi}{3}\right) & -\frac{1}{2}L_A - L_B cos2(\theta_r + \pi) \\ -\frac{1}{2}L_A - L_B cos2\left(\theta_r + \frac{\pi}{3}\right) & -\frac{1}{2}L_A - L_B cos2(\theta_r + \pi) & L_{ls} + L_A - L_B cos2\left(\theta_r + \frac{2\pi}{3}\right) \end{bmatrix} \tag{3.2.7}$$

by above equations we can express the self and mutual inductance of the damper windings. The inductance matrices L_{sr} and L_r may be expressed

$$L_{sr} = \begin{bmatrix} L_{skq1}cos\theta_r & L_{skq2}cos\theta_r & L_{sfd}sin\theta_r & L_{skd}sin\theta_r \\ L_{skq1}cos\left(\theta_r - \frac{2\pi}{3}\right) & L_{skq2}cos\left(\theta_r - \frac{2\pi}{3}\right) & L_{sfd}sin\left(\theta_r - \frac{2\pi}{3}\right) & L_{skd}sin\left(\theta_r - \frac{2\pi}{3}\right) \\ L_{skq1}cos\left(\theta_r + \frac{2\pi}{3}\right) & L_{skq2}cos\left(\theta_r + \frac{2\pi}{3}\right) & L_{sfd}sin\left(\theta_r - \frac{2\pi}{3}\right) & L_{skd}sin\left(\theta_r + \frac{2\pi}{3}\right) \end{bmatrix} \tag{3.2.8}$$

$$L_r = \begin{bmatrix} L_{lkq1} + L_{mkq1} & L_{kq1kq2} & 0 & 0 \\ L_{kq1kq2} & L_{lkq2} + L_{mkq2} & 0 & 0 \\ 0 & 0 & L_{lfd} + L_{mfd} & L_{ldkd} \\ 0 & 0 & L_{fdkd} & L_{lkd} + L_{mkd} \end{bmatrix} \tag{3.2.9}$$

In the above equations $L_A > L_B$ and L_B is zero for round rotor machine. The leakage inductances are denoted wit l in the subscript. The subscripts skq1, skq2, skd and skd in eq. (3.2.7) denoted as mutual inductance between stator and rotor windings.

The magnetizing inductance are defined as

$$L_{ma} = \frac{3}{2}(L_A - L_B) \tag{3.2.10}$$

$$L_{md} = \frac{3}{2}(L_A + L_B) \tag{3.2.11}$$

Whereas

$$L_{skq1} = \left(\frac{N_{kq1}}{N_s}\right)\left(\frac{2}{3}\right) L_{mq} \tag{3.2.12}$$

$$L_{skq2} = \left(\frac{N_{kq2}}{N_s}\right)\left(\frac{2}{3}\right) L_{mq} \tag{3.2.13}$$

$$L_{sfd} = \left(\frac{N_{fd}}{N_s}\right)\left(\frac{2}{3}\right) L_{md} \tag{3.2.14}$$

$$L_{skd} = \left(\frac{N_{kd}}{N_s}\right)\left(\frac{2}{3}\right) L_{md} \tag{3.2.15}$$

$$L_{mkq1} = \left(\frac{N_{kq1}}{N_s}\right)^2\left(\frac{2}{3}\right) L_{mq} \tag{3.2.16}$$

$$L_{mkq2} = \left(\frac{N_{kq2}}{N_s}\right)^2\left(\frac{2}{3}\right) L_{mq} \tag{3.2.17}$$

$$L_{mfd} = \left(\frac{N_{fd}}{N_s}\right)^2\left(\frac{2}{3}\right) L_{md} \tag{3.2.18}$$

$$L_{kq1kq2} = \left(\frac{N_{kq2}}{N_{kq1}}\right)^2 L_{mkq1} \tag{3.2.19}$$

$$L_{kq1kq2} = \left(\frac{N_{kq1}}{N_{kq2}}\right)^2 L_{mkq2} \tag{3.2.20}$$

$$L_{fdkd} = \left(\frac{N_{kd}}{N_{fd}}\right)^2 L_{mfd} \tag{3.2.21}$$

$$L_{fdkd} = \left(\frac{N_{fd}}{N_{kd}}\right)^2 L_{mkd} \tag{3.2.22}$$

It is convenient to incorporate the following substitute variables which refer the rotor variables to the stator windings.

$$i'_j = \left(\frac{N_j}{N_s}\right)^2\left(\frac{2}{3}\right) i_j \tag{3.2.23}$$

$$v'_j = \left(\frac{N_s}{N_j}\right)^2 v_j \tag{3.2.24}$$

$$\lambda'_j = \left(\frac{N_j}{N_s}\right)^2 \lambda_j \tag{3.2.25}$$

Where j may be the kq1, kq2, fd or kd.

The flux linkage may now be written

$$\begin{bmatrix}\lambda_{abcs}\\ \lambda'_{dqr}\end{bmatrix}=\begin{bmatrix}L_s & L'_{sr}\\ \frac{2}{3}(L'_{sr})^T & L'_r\end{bmatrix}\begin{bmatrix}-i_{abcs}\\ i'_{dqr}\end{bmatrix} \tag{3.2.26}$$

And L_s is defined by

$$L_s=\begin{bmatrix} L_{ls}+L_A-L_B cos2\theta_r & -\frac{1}{2}L_A-L_B cos2\left(\theta_r-\frac{\pi}{3}\right) & -\frac{1}{2}L_A-L_B cos2\left(\theta_r+\frac{\pi}{3}\right)\\ -\frac{1}{2}L_A-L_B cos2\left(\theta_r-\frac{\pi}{3}\right) & L_{ls}+L_A-L_B cos2\left(\theta_r-\frac{2\pi}{3}\right) & -\frac{1}{2}L_A-L_B cos2(\theta_r+\pi)\\ -\frac{1}{2}L_A-L_B cos2\left(\theta_r+\frac{\pi}{3}\right) & -\frac{1}{2}L_A-L_B cos2(\theta_r+\pi) & L_{ls}+L_A-L_B cos2\left(\theta_r+\frac{2\pi}{3}\right)\end{bmatrix} \tag{3.2.27}$$

And L_{sr} is defined by

$$L_{sr}=\begin{bmatrix} L_{mq}cos\theta_r & L_{mq}cos\theta_r & L_{md}sin\theta_r & L_{md}sin\theta_r\\ L_{mq}cos\left(\theta_r-\frac{2\pi}{3}\right) & L_{mq}cos\left(\theta_r-\frac{2\pi}{3}\right) & L_{md}sin\left(\theta_r-\frac{2\pi}{3}\right) & L_{md}sin\left(\theta_r-\frac{2\pi}{3}\right)\\ L_{mq}cos\left(\theta_r+\frac{2\pi}{3}\right) & L_{mq}cos\left(\theta_r+\frac{2\pi}{3}\right) & L_{md}sin\left(\theta_r+\frac{2\pi}{3}\right) & L_{md}sin\left(\theta_r+\frac{2\pi}{3}\right)\end{bmatrix} \tag{3.2.28}$$

$$L'_r=\begin{bmatrix} L'_{lkq1}+L_{mq} & L_{mq} & 0 & 0\\ L_{mq} & L'_{lkq2}+L_{mq} & 0 & 0\\ 0 & 0 & L'_{lfd}+L_{md} & L_{ld}\\ 0 & 0 & L_{md} & L'_{lkd}+L_{md}\end{bmatrix} \tag{3.2.29}$$

The voltage equations expressed in terms of machine variable referred to the stator windings are

$$\begin{bmatrix}v_{abcs}\\ v'_{dqr}\end{bmatrix}=\begin{bmatrix}r_s+pL_s & pL'_{sr}\\ \frac{2}{3}(L'_{sr})^T & r'_r+pL'_r\end{bmatrix}\begin{bmatrix}-i_{abcs}\\ i'_{dqr}\end{bmatrix} \tag{3.2.30}$$

$$r'_j=\left(\frac{N_s}{N_j}\right)^2\left(\frac{3}{2}\right)r_j \tag{3.2.31}$$

$$L'_{lj}=\left(\frac{N_s}{N_j}\right)^2\left(\frac{3}{2}\right)L_{lj} \tag{3.2.32}$$

Where again, j may be kq1, kq2, fd or kd.

The voltage equations given above are valid for the positive direction of stator current assumed out of the stator terminals[22].

3.2.1.1 TORQUE EQUATION IN MACHINE VARIABLES

The energy stored in the coupling field of a synchronous machine may be expressed

$$W_f = \frac{1}{2}(i_{abc})^T(L_s - L_{ls}I)i_{abcs} - (i_{abcs})^T L'_{sr} i'_{qdr} + \frac{1}{2}(\frac{3}{2})(i'_{dqr})^T(L'_r - L'_{lr}I)i'_{dqr} \quad (3.2.33)$$

Where I is the identity matrix and

$$L'_{lr} = diag[L'_{lkq1} \quad L'_{lkq2} \quad L'_{lfd} \quad L'_{lkd}] \quad (3.2.34)$$

Since the magnetic system is assumed is assumed to be linear, $W_f = W_c$ and second entry may be used with the factor P/2 included to the account for P-pole machine and a negative sign to make T_e positive for generator action thus

$$T_e = \left(\frac{P}{2}\right)\left\{-\frac{1}{2}(i_{abcs})^T \frac{\partial}{\partial\theta_r}[L_s - L_{ls}I]i_{abcs} + (i_{abcs})^T \frac{\partial}{\partial\theta_r}[L'_{sr}]i'_{qdr}\right\} \quad (3.2.35)$$

The torque and rotor speed are related by

$$T_e = -J\left(\frac{2}{P}\right)pw_r + T_p \quad (3.2.36)$$

$$\frac{P(T_p - T_e)}{2J} = pw_r \quad (3.2.37)$$

Where J is the inertia expressed in kilogram meters^2 (kg.m^2) or joule seconds^2 (J.s^2). Often the inertia is given as WR^2 in unit's pound mass feet^2. The input torque T_p is positive for a torque input to the shaft of the synchronous machine. The two mechanical state variables are w_r, rotor speed and δ, angle. So rotor angle δ is,

$$\frac{d\delta}{dt} = w_s - w_r \quad (3.2.38)$$

3.2.2 THE d–q VARIABLE MODEL

The main aim of the *d–q* model is to eliminate the dependence of inductances on rotor position. To do so, the system of coordinates should be attached to the machine part that has magnetic saliency, the rotor for SGs.

The *d–q* model should express both stator and rotor equations in rotor reference, aligned to rotor *d* and *q* axis because, with the cross saturation is neglected, there is no coupling

between the two axis[23]. The rotor windings *f, D, Q* are already aligned along *d* and *q* axes. The rotor circuit voltage equations were written in rotor coordinates.

The voltage equation of the stator winding of a synchronous machine can be expressed in arbitrary reference frame. In particular, by using the results of the voltage equations for stator winding may be written in arbitrary reference frame as

$$V_{qdos} = -r_s i_{qdos} + \omega\lambda_{dqs} + p\lambda_{dqos} \tag{3.2.39}$$

$$(\lambda_{dqs})^T = [\lambda_{ds} \; -\lambda_{qs} \; 0] \tag{3.2.40}$$

The rotor reference frame, the rotor voltage equation is

$$v''^{r}_{qdr} = r'_r i''^{r}_{qdr} + p\lambda'^{r}_{qdr} \tag{3.2.41}$$

For linear magnetic system, the flux linkage equations may be expressed with the transformation of stator variables to the arbitrary reference frame incorporated

$$\begin{bmatrix} \lambda_{qdos} \\ \lambda'^{r}_{qdr} \end{bmatrix} = \begin{bmatrix} K_s L_s (K_s)^T & K_s L'_{sr} \\ \frac{2}{3}(L'_{sr})^T (K_s)^{-1} & L'_r \end{bmatrix} \begin{bmatrix} -i_{qdos} \\ i'^{r}_{qdr} \end{bmatrix} \tag{3.2.42}$$

$$K_s L'_{sr} = \begin{bmatrix} L_{mq}cos(\theta - \theta_r) & L_{mq}cos(\theta - \theta_r) & -L_{md}sin(\theta - \theta_r) & -L_{md}sin(\theta - \theta_r) \\ L_{mq}sin(\theta - \theta_r) & L_{mq}sin(\theta - \theta_r) & L_{md}cos(\theta - \theta_r) & L_{md}cos(\theta - \theta_r) \\ 0 & 0 & 0 & 0 \end{bmatrix} \tag{3.2.43}$$

The sinusoidal term of above equations are constant, independent of ω and ω_r only if $\omega = \omega_r$. Similarly, $K_s L_s (K_s)^{-1}$ and $\frac{2}{3}(L'_{sr})^T (K_s)^{-1}$ are constant only if $\omega = \omega_r$. Therefore the time varying inductances are eliminated from the voltage equations only if the reference frame is fixed in the rotor. Hence it would appear that only the rotor reference frame is useful in the analysis of synchronous machines. It is necessary to relate the arbitrary reference frame variables to the variables in the rotor reference frame[24].

$$f^r_{qdos} = K^r f_{qdos} \tag{3.2.44}$$

$$K^r = \begin{bmatrix} \cos(\theta_r - \theta) & -\sin(\theta_r - \theta) & 0 \\ \sin(\theta_r - \theta) & \cos(\theta_r - \theta) & 0 \\ 0 & 0 & 1 \end{bmatrix} \tag{3.2.45}$$

Voltage equations in rotor reference frame variables- park's equations

Park [20] was the first to incorporate a change of variables in the analysis of synchronous machine. He transformed the stator variables to the rotor reference frame which eliminates the time-varing inductance in the voltage equations. Parks' equations are obtained by setting the speed of the arbitrary reference frame equal to the rotor speed ($\omega = \omega_r$) thus

$$v''^{r}_{qdos} = -r_s i^{r}_{qdos} + w_r \lambda^{r}_{dqs} + p\lambda'^{r}_{qdos} \tag{3.2.46}$$

$$v''^{r}_{qdr} = r'_r i''^{r}_{qdr} + p\lambda'^{r}_{qdr} \tag{3.2.47}$$

For magnetically linear system, the flux linkage may be expressed in the rotor reference frame by setting $(\theta - \theta_r)$ and whereupon Ks becomes K_s^r thus

$$\begin{bmatrix} \lambda^{r}_{qdos} \\ \lambda'^{r}_{qdr} \end{bmatrix} = \begin{bmatrix} K_s^r L_s (K_s^r)^T & K_s^r L'_{sr} \\ \frac{2}{3}(L'_{sr})^T (K_s^r)^{-1} & L'_r \end{bmatrix} \begin{bmatrix} -i^{r}_{qdos} \\ i'^{r}_{qdr} \end{bmatrix} \tag{3.2.48}$$

Using trigonometric identities

$$K_s^r L_s (K_s^r)^{-1} = \begin{vmatrix} L_{ls} + L_{mq} & 0 & 0 \\ 0 & L_{ls} + L_{md} & 0 \\ 0 & 0 & L_{ls} \end{vmatrix} \tag{3.2.49}$$

$$K_s^r L'_s = \begin{vmatrix} L_{mq} & L_{mq} & 0 & 0 \\ 0 & 0 & L_{md} & L_{md} \\ 0 & 0 & 0 & 0 \end{vmatrix} \tag{3.2.50}$$

Park's voltage equations are often written in expanded form thus

$$v^{r}_{qs} = -r_s i^{r}_{qs} + w_s \lambda^{r}_{ds} + p\lambda^{r}_{qs} \tag{3.2.51}$$

$$v^{r}_{ds} = -r_s i^{r}_{ds} + w_s \lambda^{r}_{qs} + p\lambda^{r}_{ds} \tag{3.2.52}$$

$$v''^{r}_{kq1} = r'_{kq1} i^{r}_{kq1} + p\lambda''^{r}_{kq1} \tag{3.2.53}$$

$$v''^{r}_{kq2} = r'_{kq2} i^{r}_{kq2} + p\lambda''^{r}_{kq2} \tag{3.2.54}$$

$$v''^{r}_{fd} = r'_{fd} i''^{r}_{fd} + p\lambda''^{r}_{fd} \tag{3.2.55}$$

$$v''^{r}_{kd} = r'_{kd} i''^{r}_{kd} + p\lambda''^{r}_{kd} \tag{3.2.56}$$

Flux linkage equations

$$\lambda_{qs}^{r} = -L_{ls} i_{qs}^{r} + L_{mq}(-i_{qs}^{r} + i''^{r}_{kq1}) \quad (3.2.57)$$

$$\lambda_{ds}^{r} = -L_{ls} i_{ds}^{r} + L_{md}(-i_{ds}^{r} + i'^{r}_{kd1} + i''^{r}_{fd}) \quad (3.2.58)$$

$$\lambda_{kq1}^{r} = -L_{lkq1} i_{kq1}^{r} + L_{mq}(-i_{qs}^{r} + i''^{r}_{kq1}) \quad (3.2.59)$$

$$\lambda_{kq2}^{r} = -L_{lkq2} i_{kq2}^{r} + L_{mq}(-i_{qs}^{r} + i''^{r}_{kq1}) \quad (3.2.60)$$

$$\lambda''^{r}_{fd} = L'_{lfd} i_{fd}^{r} + L_{md}(-i_{ds}^{r} + i''^{r}_{fd}) \quad (3.2.61)$$

$$\lambda''^{r}_{kd} = L'_{lkd} i_{kd}^{r} + L_{md}(-i_{ds}^{r} + i''^{r}_{fd}) \quad (3.2.62)$$

The voltage and flux linkage equations have equivalent circuit shown in Fig.3.2.

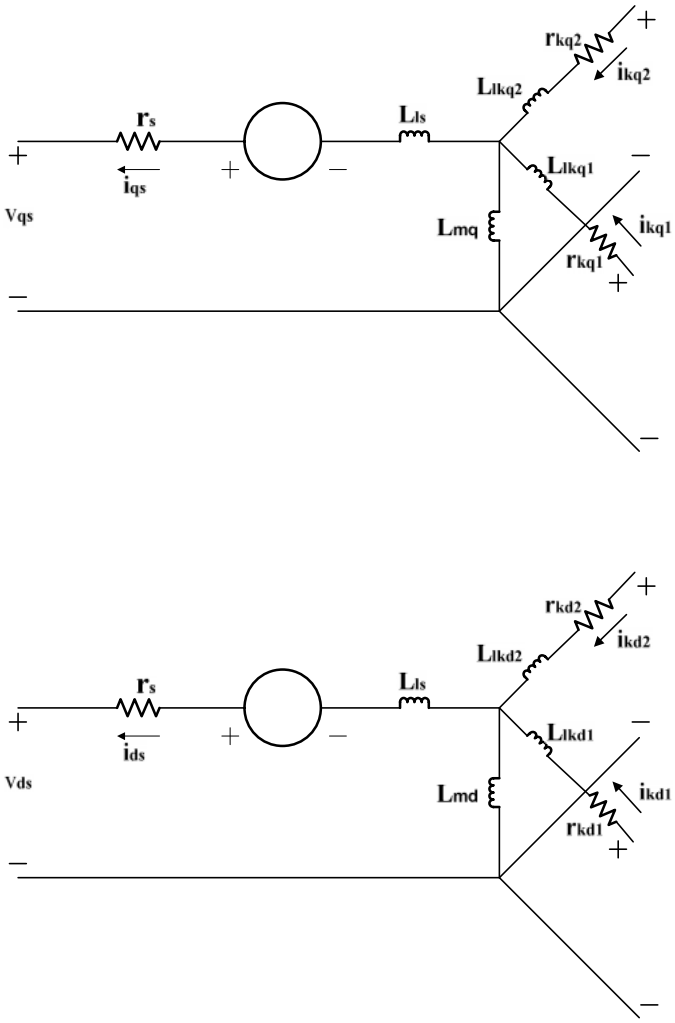

Figure 3.2: Equivalent circuit of generator in reference frame.

3.2.2.1 TORQUE EQUATION

The expression for the electromagnetic torque in terms of rotor reference-frame variable may be obtained by substituting the equation of transformation.

$$T_e = \left(\frac{P}{2}\right)[(K_s^r)^{-1} i'_{qdos}]^T \left\{-\frac{1}{2}\frac{\partial}{\partial\theta_r}[L_s - L_{ls}I](K_s^r)^{-1} i'_{qdos} + \frac{\partial}{\partial\theta_r}[L'_{sr}] i'_{qdr}\right\} \quad (3.2.63)$$

Above equation is equivalent to

$$T_e = \left(\frac{3}{2}\right)\left(\frac{P}{2}\right)(\lambda_{ds}^r i_{qs}^r - \lambda_{qs}^r i_{ds}^r) \quad (3.2.64)$$

In term of flux linkage per second and currents

$$T_e = \left(\frac{3}{2}\right)\left(\frac{P}{2}\right)\left(\frac{1}{\omega_b}\right)(\lambda_{ds}^r i_{qs}^r - \lambda_{qs}^r i_{ds}^r) \quad (3.2.65)$$

3.2.3 d-q MODEL NEGLECTING STATOR TRANSIENTS

The $p\lambda_q$ and $p\lambda_d$ terms represent the stator transients. With these terms neglected, the stator quantities contain only fundamental frequency components and the stator voltage equations appear as algebraic equations[25]. This allows the use of steady-state relationship for represents the interconnecting transmission network. The Park's voltage eq. (3.2.51, 3.2.52) can rearrange as

$$p\lambda_{qs} = v_{qs} + i_{qs}r_s - w_s\lambda_{ds} \quad (3.2.66)$$

$$p\lambda_{ds} = v_{ds} + i_{ds}r_s - w_s\lambda_{qs} \quad (3.2.67)$$

When neglecting the stator transients in the *d–q* model, it means to make $p\lambda_{ds} = 0$ and $p\lambda_{qs} = 0$ [23].There are following assumptions to simplifies the machine model significantly, to ignore transient saliency

- Both stator transients are equal ($X'_d = X'_q$).
- The flux linkage λ_{1q}(associated with the q-axis rotor circuit corresponding to X'_q also remain constant.
- The voltage behind the transient's impendence $R_a + jX'_d$ has a constant magnitude.

So after neglecting stator transients

$$v_{qs} + i_{qs}r_s - w_s\lambda_{ds} = 0 \quad (3.2.68)$$

$$v_{ds} + i_{ds}r_s - w_s\lambda_{qs} = 0 \quad (3.2.69)$$

The d-and q-axis equivalent circuits with one circuit in each axis are shown below in Fig. 3.2 and 3.3.

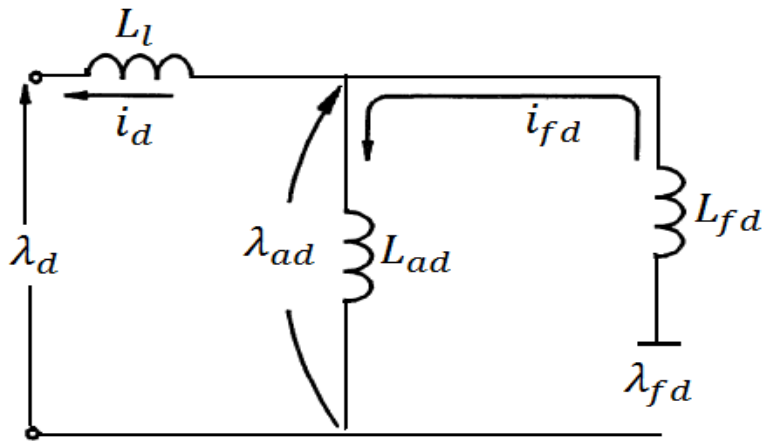

Figure 3.3: The d- axis equivalent circuit with one rotor circuit in each axis.

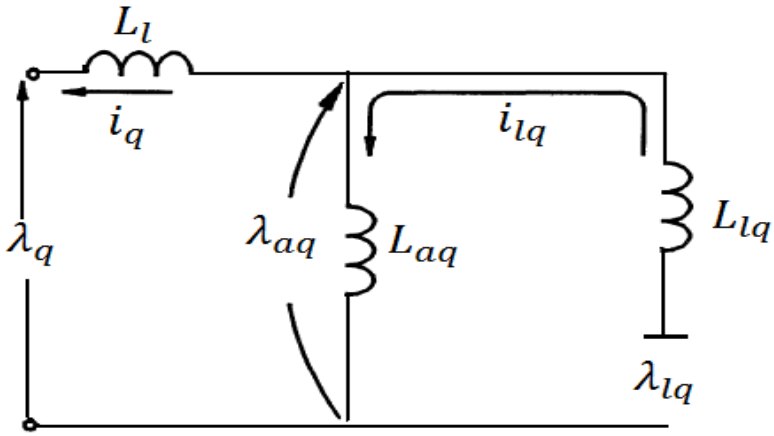

Figure 3.4: The q- axis equivalent circuit with one rotor circuit in each axis.

$$\lambda_{ad} = -L_{ad}i_d + L_{ad}i_{fd} \quad (3.2.70)$$

$$\lambda_d = \lambda_{ad} - L_l i_d \quad (3.2.71)$$

$$\lambda_{fd} = \lambda_{ad} + L_{fd}i_{fd} \quad (3.2.72)$$

From above equation

$$i_{fd} = \frac{\lambda_{fd} - \lambda_{ad}}{L_{fd}} \tag{3.2.73}$$

Substituting in equation (3.2.66), it gives

$$\lambda_{ad} = -L_{ad} i_d + \frac{L_{ad}}{L_{fd}} \left(\lambda_{fd} - \lambda_{ad} \right) \tag{3.2.74}$$

Rearranging to express λ_{ad} in terms of λ_{fd}, we find

$$\lambda_{ad} = L'_{ad} \left(-i_d + \frac{\lambda_{fd}}{L_{fd}} \right) \tag{3.2.75}$$

Where

$$L'_{ad} = \frac{1}{\frac{1}{L_{ad}} + \frac{1}{L_{fd}}} = L'_d - L_l \tag{3.2.76}$$

Similarly, for the q-axis

$$\lambda_{aq} = L'_{aq} \left(-i_q + \frac{\lambda_{fq}}{L_{lq}} \right) \tag{3.2.77}$$

$$L_{aq} = L'_d - L_l \tag{3.2.78}$$

The q-axis stator voltage is given by

$$v_d = -r_a i_d - \omega \lambda_q \tag{3.2.79}$$

$$v_d = -r_a i_d + \omega (L_l i_q - \lambda_{aq}) \tag{3.2.80}$$

Where $\omega = \omega_r = \omega_0 = 1.0\, pu$. Substituting for λ_{aq} from above equation (3.2.77) gives

$$v_d = -r_a i_d + \omega L_l i_q - \omega L'_{aq} \left(-i_q + \frac{\lambda_{1q}}{L_{lq}} \right) \tag{3.2.81}$$

$$v_d = -r_a i_d + \omega (L_l + L'_{aq}) i_q - \omega L'_{aq} \left(\frac{\lambda_{1q}}{L_{lq}} \right) \tag{3.2.82}$$

$$v_d = -r_a i_d + x'_q i_q + E'_d \tag{3.2.83}$$

$$v_d = -v_0 sin\delta + r_e i_d + x_e i_q \tag{3.2.84}$$

Where

$$E'_d = -\omega L'_{aq}\left(\frac{\lambda_{1q}}{L_{lq}}\right) \quad (3.2.85)$$

Similarly, the q-axis stator voltage is given by

$$v_q = -r_a i_q + x'_d i_d + E'_q \quad (3.2.86)$$

$$v_q = v_0 cos\delta + r_e i_q \quad (3.2.87)$$

Where

$$E'_q = -\omega L'_{ad}\left(\frac{\lambda_{fd}}{L_{fd}}\right) \quad (3.2.88)$$

By neglecting the amortisseur effects the machine model can be simplified. This minimizes the data requirements since the machine parameters related to the amortisseures are often not readily available[26][27]. With the amortisseure neglected the stator voltage equations are

$$v_d = -\lambda_q - r_a i_d \quad (3.2.89)$$

$$v_q = -\lambda_d - r_a i_q \quad (3.2.90)$$

Rotor voltage equations

$$v_{fd} = p\lambda_{fd} - r_{fd} i_{fd} \quad (3.2.91)$$

$$p\lambda_{fd} = v_{fd} - r_{fd} i_{fd} \quad (3.2.92)$$

Flux linkage equation

$$\lambda_d = -X_d i_d + X_{ad} i_{fd} \quad (3.2.93)$$

$$\lambda_q = -X_q i_q \quad (3.2.94)$$

$$\lambda_{fd} = -X_{ad} i_d + X_{ffd} i_{fd} \quad (3.2.95)$$

$$E_I = X_{ad} i_{fd} \quad (3.2.96)$$

$$E'_q = \frac{X_{ad}}{X_{ffd}}\lambda_{fd} \quad (3.2.97)$$

$$E_{fd} = \frac{X_{ad}}{R_{fd}}\, e_{fd} \quad (3.2.98)$$

Multiplied the equation (3.2.97) by $\frac{X_{ad}}{X_{ffd}}$

$$E'_q = \frac{X_{ad}^2}{X_{ffd}} i_{fd} + E_I \quad (3.2.99)$$

Whereas

$$X'_d = X_l + \frac{X_{ad}X_{fd}}{X_{ad}+X_{fd}} \quad (3.2.100)$$

$$X'_d = (X_d - X_{ad}) + \frac{X_{ad}X_{fd}}{X_{ad}+X_{fd}} \quad (3.2.101)$$

$$X'_d = X_d - \frac{X_{ad}^2}{X_{ffd}} \quad (3.2.102)$$

Then

$$X_d - X'_d = \frac{X_{ad}^2}{X_{ffd}} \quad (3.2.103)$$

$$E'_q = E_I - (X_d - X'_d) i_d \quad (3.2.104)$$

Multiplying equation (3.2.92) by $\frac{X_{ad}}{X_{fd}}$ thought, we have

$$p\left(\frac{X_{ad}}{X_{ffd}}\lambda_{fd}\right) = \frac{X_{ad}}{R_{fd}}\frac{R_{fd}}{X_{ffd}} e_{fd} - \frac{R_{fd}}{X_{ffd}} X_{ad} i_{fd} \quad (3.2.105)$$

Above equation is express in new variables

$$pE'_q = \frac{1}{T'_{do}}(E_{fd} - E_I) \quad (3.2.106)$$

Here T'_{do} is the open-circuit transient time constant.

From equation (3.2.104),

$$pE'_q = \frac{1}{T'_{do}}(E_{fd} - (E'_q + (X_d - X'_d) i_d)) \quad (3.2.107)$$

$$pE'_q = \frac{1}{T'_{do}}(E_{fd} - E'_q + (X'_d - X_d) i_d)) \quad (3.2.108)$$

$$sE'_q = -\frac{E'_q}{T'_{do}} + \frac{1}{T'_{do}}(E_{fd} + (X'_d - X_d) i_d)) \quad (3.2.109)$$

$$E'_q\left(\frac{1+sT'_{do}}{T'_{do}}\right) = \frac{1}{T'_{do}}(E_{fd} + (X'_d - X_d) i_d)) \quad (3.2.110)$$

$$E'_q = \frac{E_{fd}}{1+sT'_{do}} + \frac{X'_d - X_d}{1+sT'_{do}} i_d \quad (3.2.111)$$

Then similarly for E'_d

$$E'_d = E_I - (X_q - X'_d) i_q \quad (3.2.112)$$

$$pE'_d = \frac{1}{T'_{qo}} (E_I) \quad (3.2.113)$$

$$E'_d = \frac{X'_d - X_q}{1+sT'_{qo}} i_q \quad (3.2.114)$$

3.2.3.1 MECHANICAL PART

If δ is the angular position of the rotor in electrical radians with respect to a generator rotating reference and δ_0 is its value at t=0

$$\delta = \omega_r t - \omega_0 t + \delta_0 \quad (3.2.115)$$

Where ω_r is the angular position of the rotor and ω_0 is its rated value. By taking time derivative, we have

$$\frac{d\delta}{dt} = \omega_r - \omega_0 = \Delta\omega_r \quad (3.2.116)$$

And

$$\frac{d^2}{dt^2}\delta = \frac{d(\Delta\omega_r)}{dt} \quad (3.2.117)$$

$$\frac{d^2}{dt^2}\delta = \omega_0 \frac{d\Delta\omega_r}{dt} \quad (3.2.118)$$

$$\frac{d\delta}{dt} = \omega_0 \Delta\omega r \quad (3.2.119)$$

$$\delta = \omega_0 \frac{\Delta\omega r}{s} \quad (3.2.120)$$

For load- frequency studies, rather than torque mechanical and electrical power is used.the relationship between P and T is

$$P = \omega_r T \quad (3.2.121)$$

The overall frequency- dependent characteristic of a composite load may be expressed as shown in Fig. 3.5.

$$\Delta P_e = \Delta P_L + D\Delta\omega_r \quad (3.2.122)$$

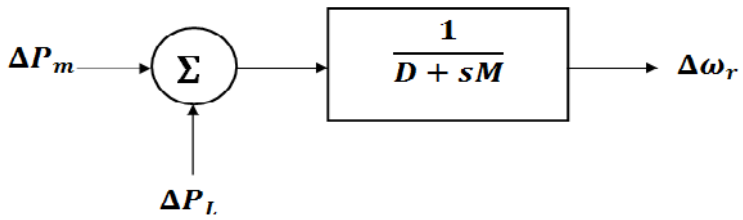

Figure 3.5: The system block diagram for the effect of the load damping

Where

ΔP_L = non frequency- sensitive load change

$D\Delta\omega_r$= frequency- sensitive load change

D= load-damping constant

$$\Delta\omega_r = \frac{1}{D+sM}(P_L - P_e) \qquad (3.2.123)$$

3.3 EXCITER MODEL

The excitation control system is an automatic feedback control having the primary function of maintaining a predetermined terminal voltage by modifying the field current of the generator based on changes in the terminal voltage. Without excitation control, terminal voltage would fluctuate as a result of changes in output power or external network conditions. The control is referred to as “negative feedback” because when terminal voltage increases, field current is decreased, and when terminal voltage decreases, field current is increased[11].

In addition, the excitation system performs control and protective functions essential to the satisfactory performance of the power system by controlling the field voltage and thereby the field current. The control functions include the control of voltage and reactive power flow, and the enhancement of system stability. The protective function ensures that the capability limits of the machine, excitation system, and other equipment are not exceeded [27].

Depending on type of excitation system, there may be many levels of excitation control system stabilization involving the major outer loop and minor inner loops. Feedback excitation system, which has been use for study Fig. 3.5.

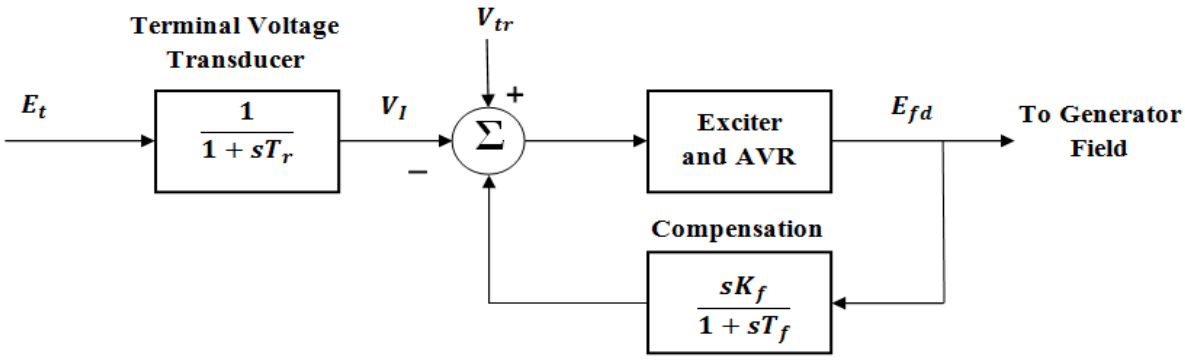

Figure 3.6: Block diagram for excitation control system

Then exciter output voltage, E_{fd}

$$E_{fd} = K_A[V_{tr} - V_t - V_s] \quad (3.3.1)$$

Here

$$V_s = \frac{sK_f}{1+sT_f} E_{fd} \quad (3.3.2)$$

$$K_A = \frac{K_E}{1+sT_E} \quad (3.3.3)$$

$$V_I = \frac{1}{1+sT_r} V_t \quad (3.3.4)$$

V_{tr} is reference voltage, V_t is terminal output voltage and V_1 is the output of terminal voltage transducer.

3.4 TURBINE MODEL

Electrical generators convert mechanical energy into electrical energy. The mechanical energy is produced by prime movers. Prime movers are mechanical machine. They convert primary energy of a fuel are fluid into mechanical energy[28]. They are also called as turbines or engines. The block diagram of the steam turbine has been modelled for study of turbine and governor system which is shown in Fig. 3.6.

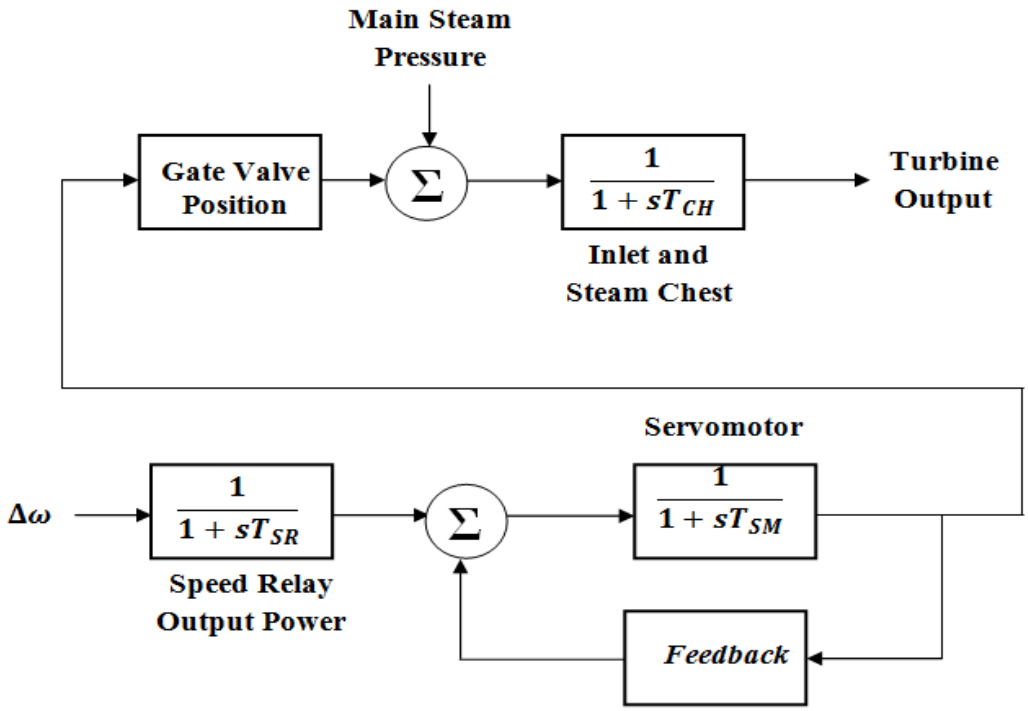

Figure 3.7: block diagram for turbine and governor control system

Governors and turbines are more important in the long-term simulation than in the transient simulations. Their response is inherently slow. However some of the governor time constants can be eliminated to produce a reduce order model for the long term simulation[29]. Output power equation for different parts of turbine and governor system.

$$\Delta P_r = \frac{K_G}{1+sT_{SR}}\Delta\omega \quad (3.4.1)$$

$$\Delta P_h = \frac{1}{1+sT_{SM}}\Delta P_r \quad (3.4.2)$$

$$\Delta P_C = \frac{1}{1+sT_{CH}}\Delta P_h \quad (3.4.3)$$

$$\Delta P_M = \frac{sK_{RH}T_{RH}}{1+sT_{RH}}\Delta P_c \quad (3.4.4)$$

3.5 POWER SYSTEM STABILIZER MODEL

To compensate the unwanted effect of voltage regulators, additional signals are introduced in feedback loop of voltage regulators. The additional signals are mostly derived from speed deviation, excitation deviation or accelerating power. This is achieved by injecting a stabilizing signal into the excitation system voltage reference

summing point junction. The device setup to provide this signal is called “power system stabilizer”. Model for power system stabilizer used for simulation study, is shown in Fig. 3.8[23]. It consists of phase-lead compensation block, a single washout block and a gain block.

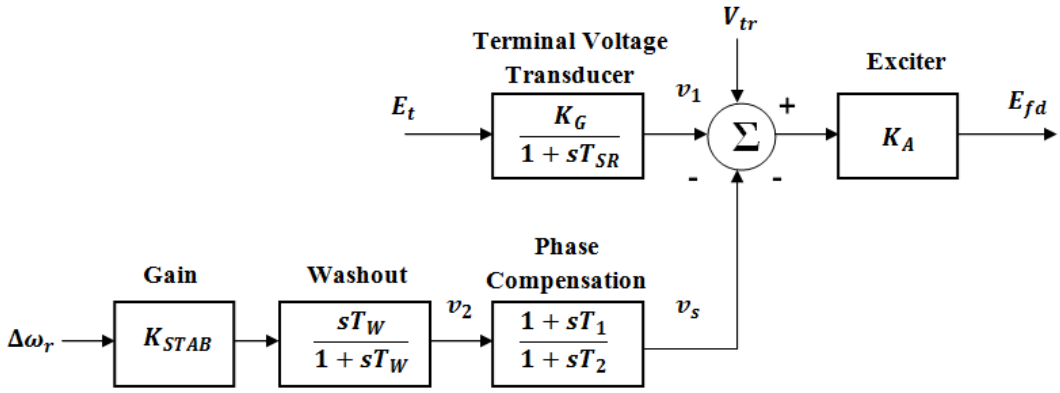

Figure 3.8: Block diagram of power system stabilizer.

The basic function of a power system stabilizer is to add damping to the generator power oscillations by controlling its excitation using an auxiliary stabilizing signal. To provide damping, the stabilizer must add a component of electrical torque in phase with rotor speed deviation. The application of power system stabilizer (PSS) is to generate a supplementary signal, which is applied to control loop of the generating unit to produce a positive damping.

The phase compensation block provides the appropriate phase lead characteristics to compensate for the phase lag between exciter input and generator electrical torque. The phase compensation may be a single first order block as shown in Figure 3.7 or having two or more first order blocks or second order blocks with complex roots.

The signal washout block serves as high pass filter, with time constant Tw high enough to allow signals associated with oscillations in ωr to pass unchanged, which removes d.c. signals. Without it, steady changes in speed would modify the terminal voltage. It allows PSS to respond only to changes in speed[30].

After block of washout from figure 3.7, using perturbed values, we have

$$\Delta v_2 = \frac{sT_W}{1+sT_W}(K_{STAB}\Delta\omega_r) \qquad (3.5.1)$$

Hence

$$p\Delta v_2 = (K_{STAB} p\Delta\omega_r) - \frac{1}{T_W}\Delta v_2 \quad (3.5.2)$$

After a block of phase compensation

$$\Delta v_s = \Delta v_2 \left(\frac{1+sT_1}{1+sT_2}\right) \quad (3.5.3)$$

Hence

$$p\Delta v_s = \frac{T_1}{T_2} p\Delta v_2 + \frac{1}{T_2}\Delta v_2 - \frac{1}{T_2}\Delta v_s \quad (3.5.4)$$

After block of exciter

$$\Delta E_{fd} = K_A(\Delta v_s - \Delta v_1) \quad (3.5.5)$$

The stabilizer gain K_{STAB} determines the amount of damping introduced by PSS. Ideally, the gain should be set at a value corresponding to maximum damping; however, it is limited by other consideration.

3.6 SIMULATION OF SUPERCODUCTING GENERATOR IN MATLAB

3.6.1 ALGORITHM FOR DIGITAL SIMULATION

STEP1: Start.

STEP2: Read the generator data.

STEP3: Calculate the initial conditions.

STEP4: Solve the first order differential equations using Runge-Kutta method.

STEP5: Compute intermediate variables.

STEP7: Check the time, if t=t_s. If not then store the variables and parameters.

STEP8: Increase the time by small step dt and go to step 4 and repeat.

STEP9: plot the graphs.

STEP9: Stop.

3.6.2 FLOW CHART FOR DIGITAL SIMULATION

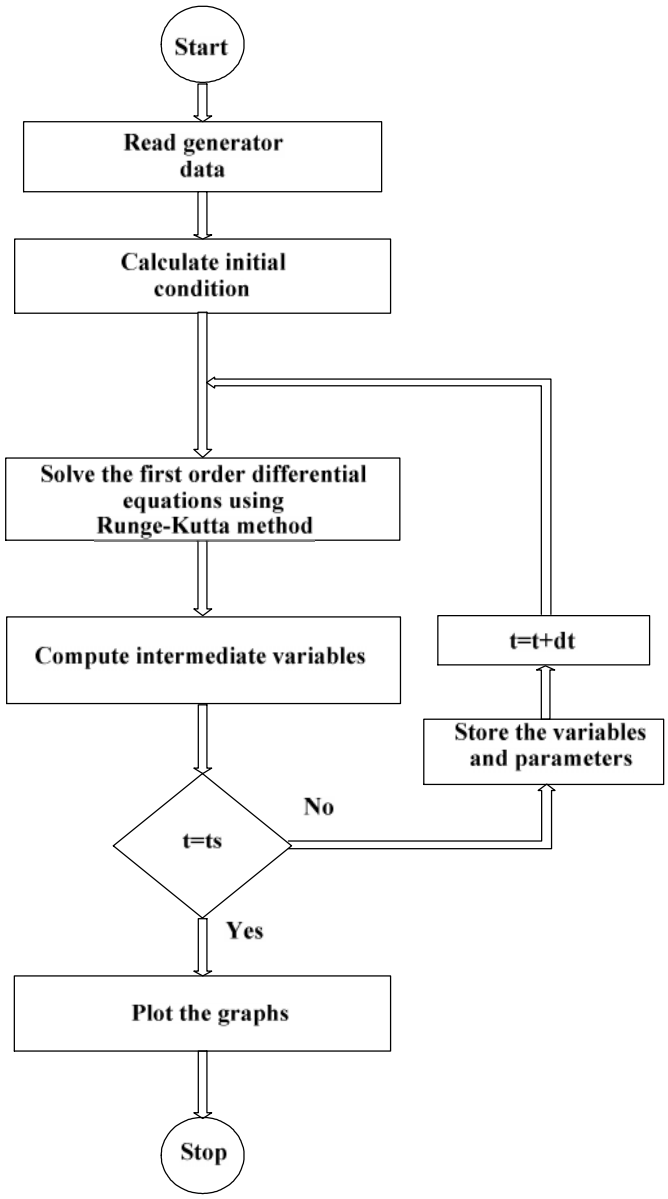

Figure 3.9: Flow chart for simulation of superconducting generator

CHAPTER 4

DIGITAL SIMULATION OF SYSTEM USING SIMULINK

4.1 GENERAL

Simulation of synchronous superconducting machine can be done using various simulation tools. But mainly MATLAB/SIMULINK and EMTP (Electromagnetic transient programs) simulation tools are used in various applications. In MATLAB these simulation analysis can be done in programming codes and by using basic function blocks in SIMULINK. To observe the dynamic performance of synchronous superconducting machine by using the differential equations are programmed in programming codes in MATLAB. But the transient analysis for synchronous superconducting machine is done in MATLAB/SIMLINK with complete detailed study of exciter circuit, turbine and governor system and power system stabilizer which is linked to an infinitive bus. The SIMULINK implementation is adopted because of its inherent integration of vector system representation in block diagram form, of numerical analysis methods. So this approach is pedagogically better than using compilation of program codes [31].

The development of SIMULINK models of drive assemblies is a relatively simple task consisting of combining input output block representation of the various components making up the system. This approach provides a powerful design tool because of the ease of observing the effects of parameter modifications and of changes in system configurations and control strategies. MATLAB offers modelling, simulation and analysis under a graphical user interface (GUI) environment. The construction of a model is simplified with click-and-drag mouse operations. SIMULINK includes a comprehensive block library of toolboxes for both linear and nonlinear analyses.

4.2 SIMULINK MODEL OF INTEGRATED SYSTEM

A model of the synchronous machine with appropriate degrees is given in this work for a transient stability investigation. The considered single machine-infinitive bus system is given in Fig. 4.1.

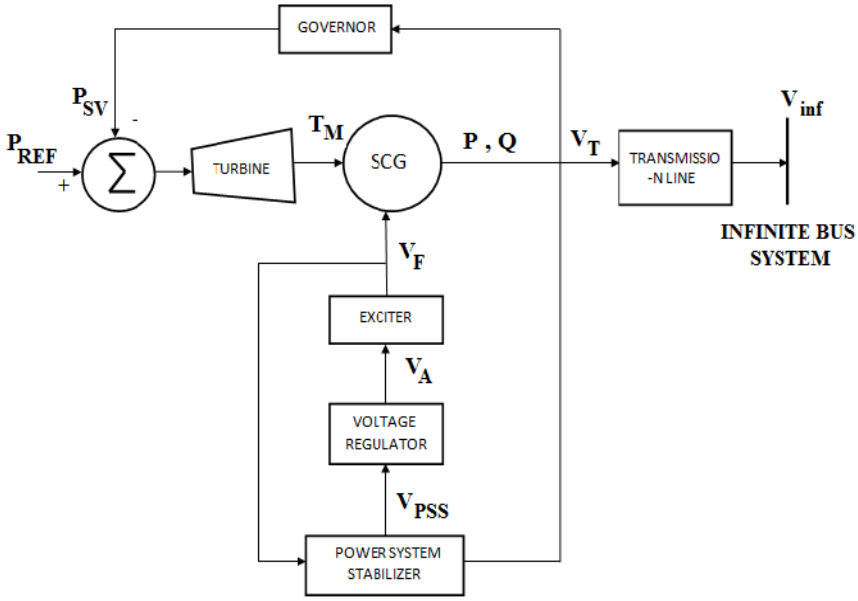

Figure 4.1: Single machine-infinitive bus system

The synchronous superconducting generator's dynamic model equations in the Laplace domain can be created by connecting appropriate function blocks. In order to simulate the detailed transient analysis of the machine, addition of new sub-models is needed to model the operation of various control functions. These sub-models are used in the calculation of various values related to the generator such as the steady state, exciter loop, turbine governor model, power system stabilizer model, voltage and the currents [32].

The complete model of the synchronous superconducting machine used in the simulation is given below in Fig. 4.2. Simulation model for the generator is constructed by using properly selected sub-blocks. These main sub blocks are

- Steady state values.
- Exciter model.
- Terminal voltage controller.
- Electrical part.
- Turbine and governor model.
- Power system stabilizer model.
- Fault

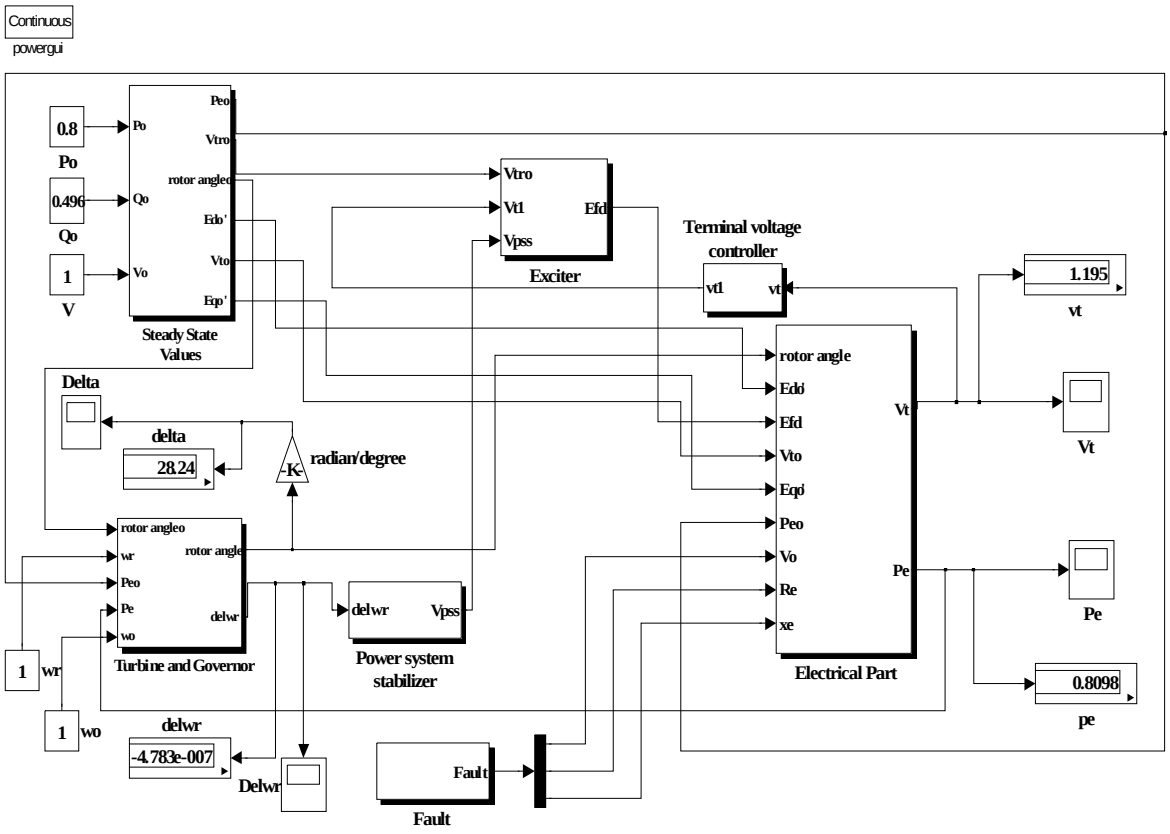

Figure 4.2: Complete model of synchronous superconducting machine

The above sub-blocks are modelled in SIMULINK. There are the following various model of the machine [33].

4.2.1 SIMULINK MODEL OF STEADY STATE VALUE

The steady state values are calculated separately according to the block diagram shown below in Fig 4.3. The function blocks given in figure which corresponds to initial values of current, load angle, rotor angle, electromotor force in the machine, terminal voltage, real power, exciter voltage, and reference terminal voltage are calculated using the equations given below

$$I_0 = \frac{\sqrt{P_0^2+Q_0^2}}{V_0} \qquad (4.2.1)$$

$$\square_0 = arctan\frac{Q_0}{P_0} \qquad (4.2.2)$$

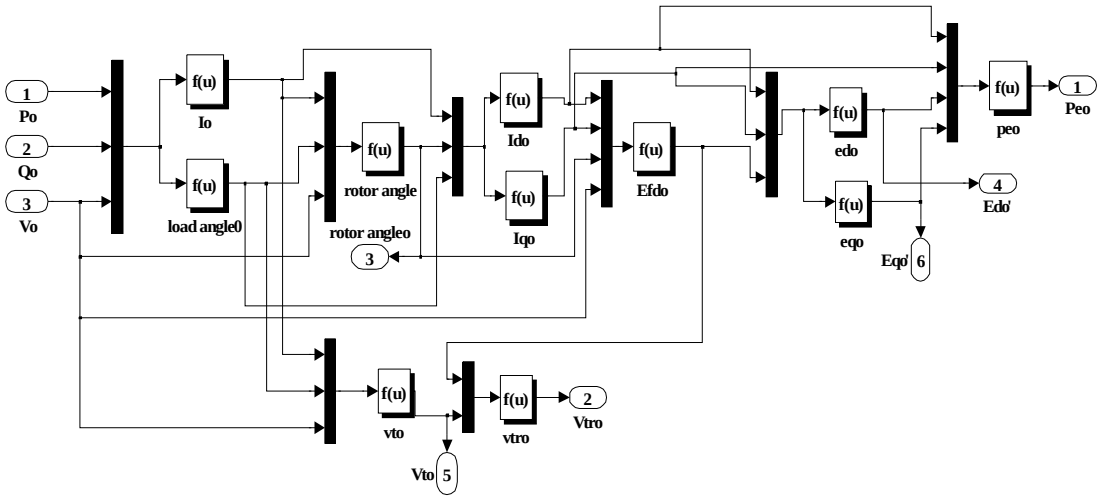

Figure 4.3: Steady state sub model

$$\delta_0 = arctan\frac{I_0(x_q+x_e)cos\emptyset_0 - I_0(R_a+R_e)sin\square_0}{V_0+I_0(R_a+R_e)cos\square_0+I_0(x_q+x_e)sin\square_0} \quad (4.2.3)$$

$$I_{do} = -I_0 \sin(\delta_0 + \square_0) \quad (4.2.4)$$

$$I_{qo} = I_0 \cos(\delta_0 + \square_0) \quad (4.2.5)$$

$$E_{fd0} = V_0 cos\delta_0 + (R_a + R_e)I_{q0} - (x_d + x_e)I_{d0} \quad (4.2.6)$$

$$V_{to} = \sqrt{(V_0 + R_e I_0 cos\square_0 + x_e I_0 sin\square_0)^2 + (x_e I_0 cos\square_0 - R_e I_0 sin\square_0)^2} \quad (4.2.7)$$

$$E'_{do} = -(x_q - x'_d)I_{qo} \quad (4.2.8)$$

$$E'_{qo} = E_{fd0} + (x_d - x'_d)I_{do} \quad (4.2.9)$$

$$P_{e0} = E'_{d0}I_{d0} + E'_{q0}I_{q0} \quad (4.2.10)$$

$$V_{tr0} = \frac{E_{fd0}}{K_E} + V_{t0} \quad (4.2.11)$$

4.2.2 SIMULINK MODEL OF EXCITER

The exciter is represented by a second-order dynamical model as in Fig. 4.4. The sub model has three inputs, V_{tr0}, V_{PSS} and V_t, reference and instantaneous values of terminal voltage and power system stabilizer voltage, respectively and one output E_{fd} in per-unit

values. E_{fd} is the output of the exciter system with one compensation feedback. The modle for exciter system has been discussed briefly in chapter 3. Whereas the values of K_E, K_f, T_f and T_E has been taken from table 5.2.

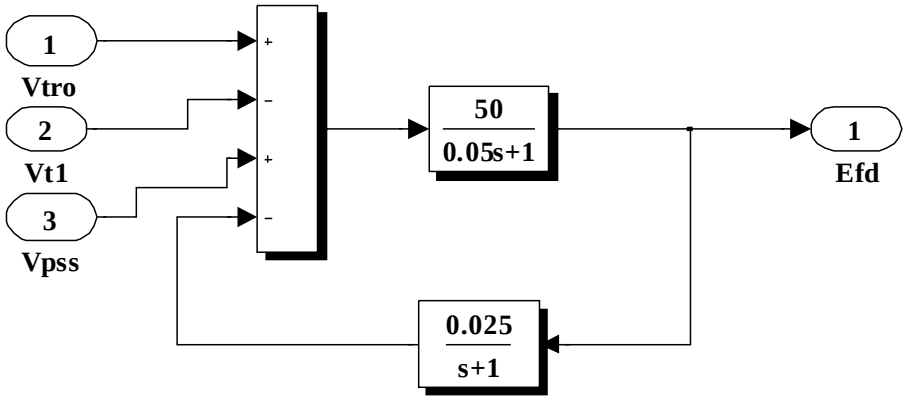

Figure 4.4: Sub model of exciter system

4.2.3 SIMULINK MODEL OF VOLTAGE CONTROLLER

The sub block of the terminal voltage transducer is shown in Fig. 4.5. It senses generator terminal voltage, rectifies and filters it to dc quantity, and compares it with a reference which represents the desired terminal voltage.

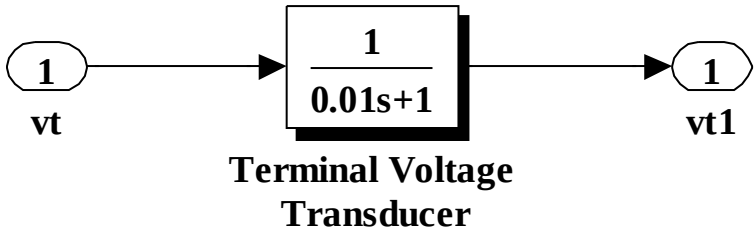

Figure 4.5: Sub model of voltage transducer

Here

$$V_{t1} = \frac{1}{1+sT_{SR}} V_t \qquad (4.2.12)$$

In above shown sub model the value of $T_{SR} = 0.01$.

4.2.4 SIMULINK MODEL OF ELECTRICAL PART

The sub-model shown in Fig. 4.6 represents continuous operation of the electrical parts of the machine. The initial values which will be used until a fault occurs are provided by two switches in the sub-model. The inputs of the sub-model are δ, E'_{do}, E_{fd} V_{to}, E'_{qo}, P_{e0}, V_o, R_e, x_e, and the outputs are V_t, P_e.

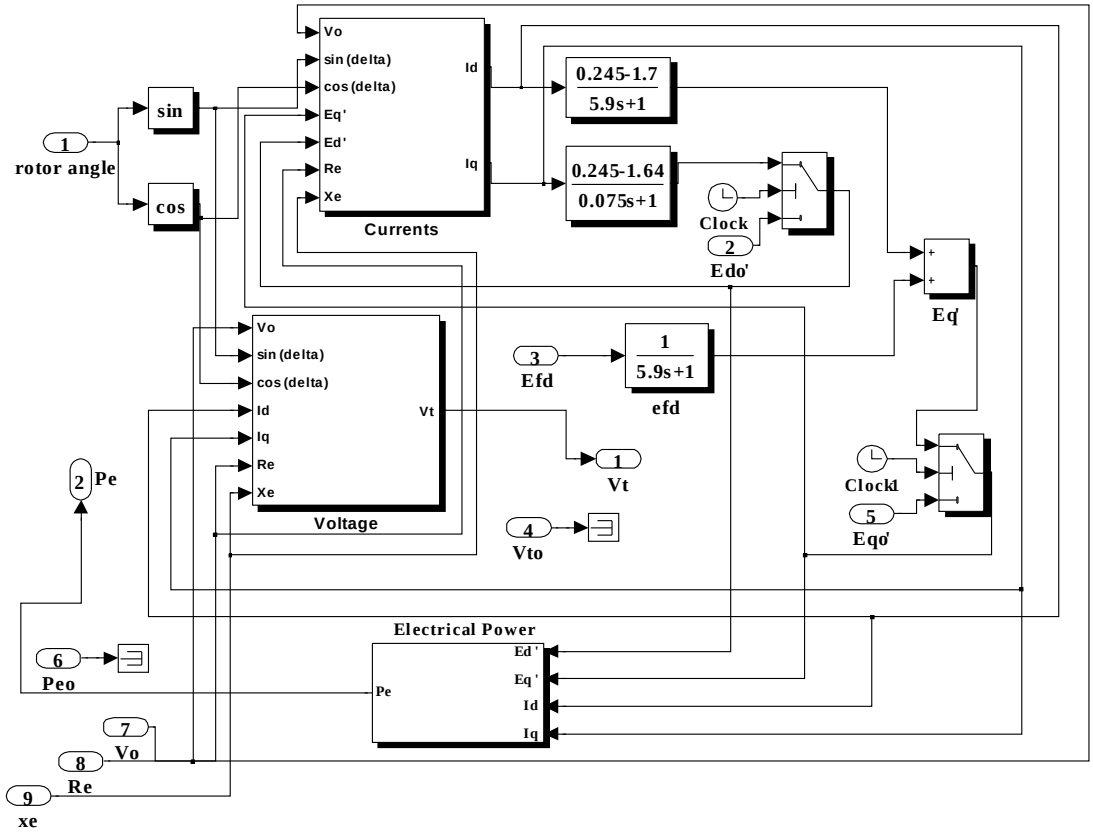

Figure 4.6: Sub model of continuous operation of electric parts

The sub-models for currents, terminal voltage and real electrical power are given in Fig. 4.7, 4.8 and 4.9 respectively. The values of currents I_d and I_q can be calculated by solving equations given below.

$$V_{td} = E'_d - R_a I_d - X'_d I_d = -V_0 sin\delta + R_e I_d + X_e I_q \qquad (4.2.13)$$

$$V_{tq} = E'_q - R_a I_q + X'_d I_d = V_0 cos\delta + R_e I_q - X_e I_d \qquad (4.2.14)$$

$$\begin{bmatrix} E'_d + V_0 sin\delta \\ E'_q - V_0 cos\delta \end{bmatrix} = \begin{bmatrix} R_a + R_e & X_e + X'_d \\ -(X_e + X'_d) & R_a + R_e \end{bmatrix} \begin{bmatrix} I_d \\ I_q \end{bmatrix} \quad (4.2.15)$$

$$E'_d + V_0 sin\delta = (R_a + R_e) I_d + (X_e + X'_d) I_q \quad (4.2.16)$$

$$E'_q - V_0 cos\delta = -(X_e + X'_d) I_d + (R_a + R_e) I_q \quad (4.2.17)$$

By solving above equations, here q-axis current (I_q)

$$I_q = \frac{(X_e + X'_d)(E'_d + V_0 sin\delta) + (R_a + R_e)(E'_q - V_0 cos\delta)}{(X_e + X'_d)^2 + (R_a + R_e)^2} \quad (4.2.18)$$

d-axis current (I_d)

$$I_d = \frac{(E'_q - V_0 cos\delta)}{-(X_e + X'_d)} - (R_a + R_e) \left(\frac{(E'_d + V_0 sin\delta) + \frac{(R_a + R_e)(E'_q - V_0 cos\delta)}{(X_e + X'_d)}}{(X_e + X'_d)^2 + (R_a + R_e)^2} \right) \quad (4.2.19)$$

Here f (u) is functions block, which is shown below in Fig. 4.7. This block is used to calculate the values of currents I_d and I_q by using the eq. (4.2.18) and (4.2.19).

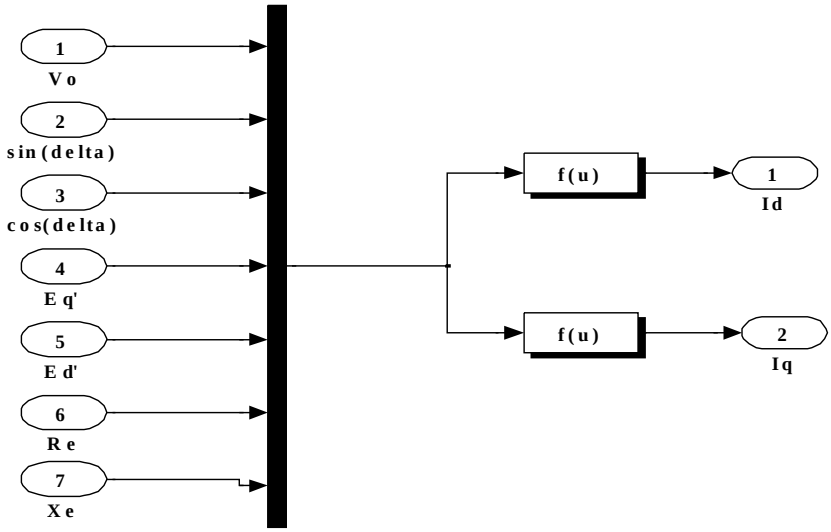

Figure 4.7: Sub model for currents

The value of the terminal voltage V_t can be calculated by using eq. (4.2.13) and (4.2.14).

$$V_{td} = -V_0 sin\delta + R_e I_d + X_e I_q \quad (4.2.20)$$

$$V_{tq} = V_0 cos\delta + R_e I_q - X_e I_d \quad (4.2.21)$$

$$V_t = \sqrt{{V_{td}}^2 + {V_{tq}}^2} \quad (4.2.22)$$

$$V_t = \sqrt{(-V_0 sin\delta + R_e I_d + X_e I_q)^2 + (V_0 cos\delta + R_e I_q + X_e I_d)^2} \quad (4.2.23)$$

In Fig. 4.8, the f (u) is functions block used to calculate the values of V_t by using eq. (4.2.23).

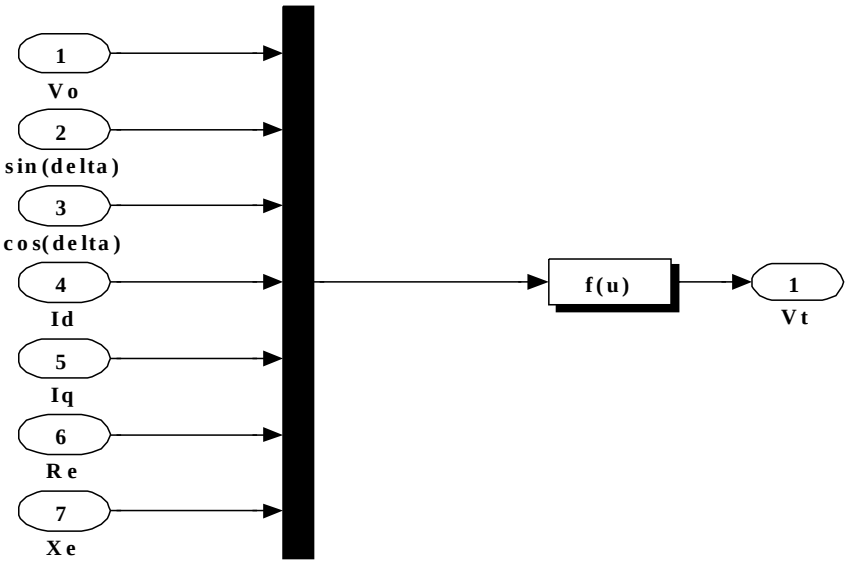

Figure 4.8: Sub model for voltage

The value of the electrical power P_e can be calculated as

$$P_e = E'_d I_d + E'_q I_q \quad (4.2.\ 24)$$

In Fig. 4.9, the f (u) is functions block used to calculate the values of P_e by using eq. (4.2.24).

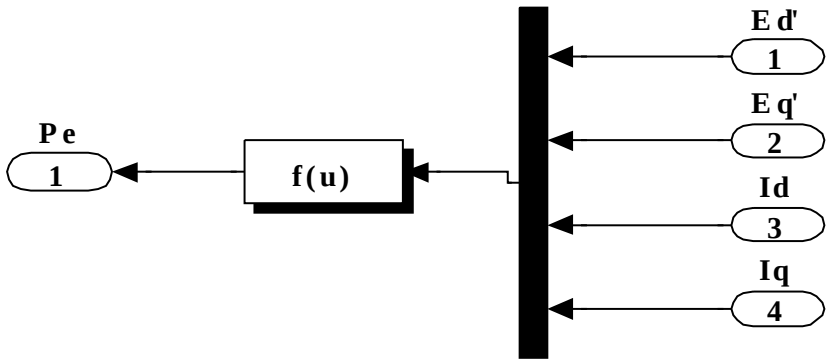

Figure 4.9: Sub model for electrical power

4.2.5 SIMULINK MODEL OF TURBINE AND GOVERNOR

The sub-model of the mechanical part is represented by a dynamical model as shown in Fig. 4.10. The considered system includes a turbine and governor sub-system and the blocks of the relations among rotor angle δ, deviation of angular speed Δw. The sub-model includes five inputs, steady state value of rotor angle in radian, reference value of angular speed, the steady state and instantaneous values of real electrical power and steady state value of angular speed, in per-unit values. It has one output rotor angle in radians.

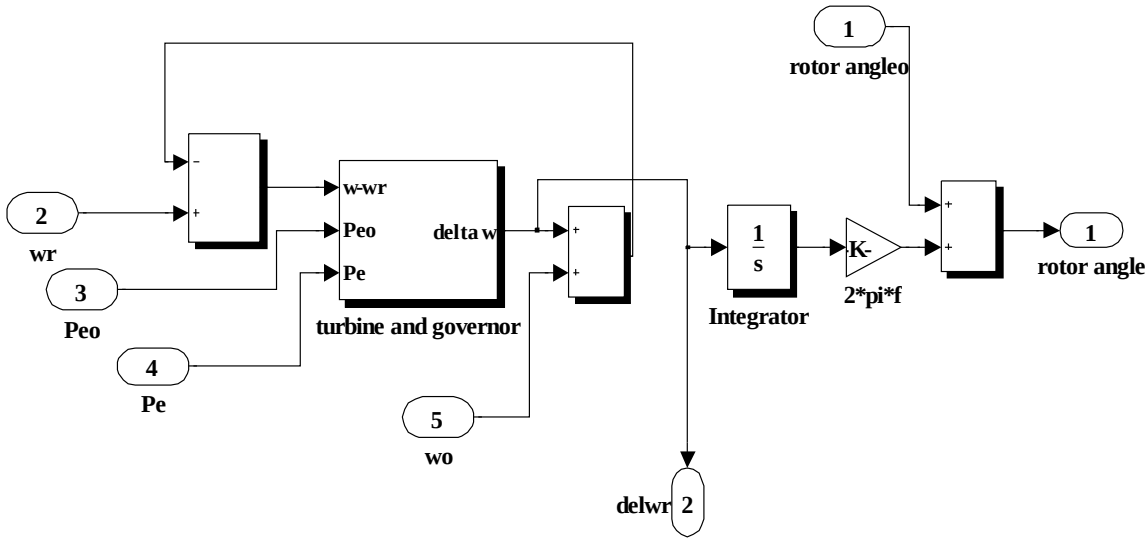

Figure 4.10: Sub model of mechanical part

The sub-model of the turbine and governor system is represented in Fig. 4.11. This sub-model contains three inputs, the difference between the reference value and instantaneous value of angular speed, the steady state value of mechanical power, instantaneous value of electrical power, in per-unit, and one output, the deviation of angular speed in per-unit.

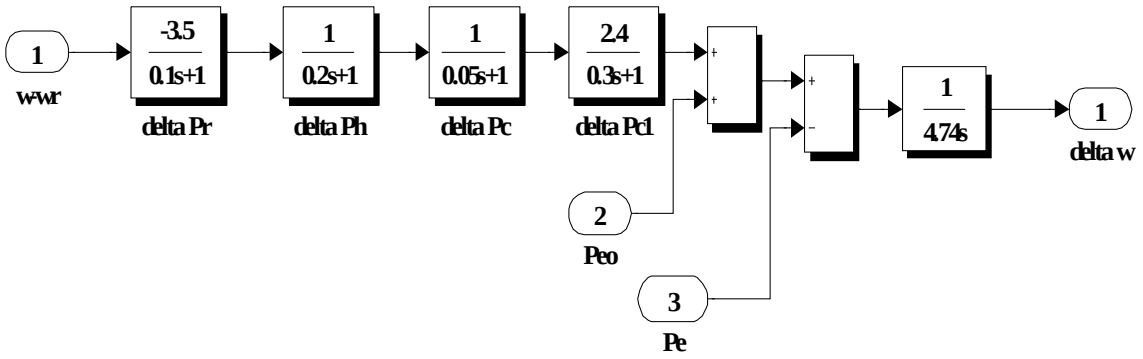

Figure 4.11: Model for turbine and governor control system

The model of turbine and governor has been discussed briefly in chapter 3. The parameters shown in Fig. 4.11 have been taken from table 5.2.

4.2.6 SIMULINK MODEL OF POWER SYSTEM STABILIZER

The sub model of power system stabilizer is shown in Fig. 4.12. Output Δw_r from the turbine and governor control system is connected with stabilizer gain and phase compensation block. Output V_{PSS} is connected as third input for the sub model of excitation control system. The model of power system stabilizer has been discussed briefly in chapter 3. The values of parameters shown in Fig.4.12 have been taken from table 5.2.

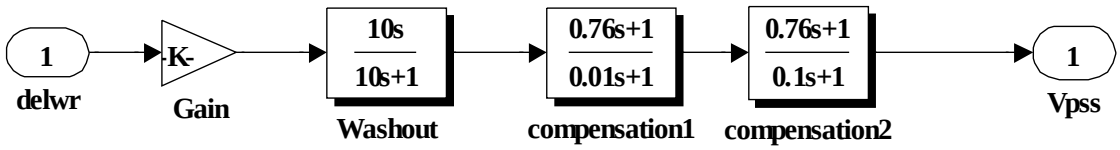

Figure 4.12: Model for power system stabilizer

$$V_{pss} = (K_{STAB}\Delta\omega_r)\frac{sT_W}{1+sT_W}\left(\frac{1+sT_1}{1+sT_2}\right)\left(\frac{1+sT_3}{1+sT_4}\right) \qquad (4.2.25)$$

4.2.7 SIMULINK MODEL OF FAULT

For transient stability analysis of a machine, it is assumed that a three-phase short-circuit at the sending terminal of one of the parallel lines has occurred at 0.6 s and the fault has continued until 0.78 s. The fault is cleared by switching the faulted line on 0.78 and then the system is returned to the pre-fault configuration. These cases are represented by switch blocks in the model given in Fig. 4.13.

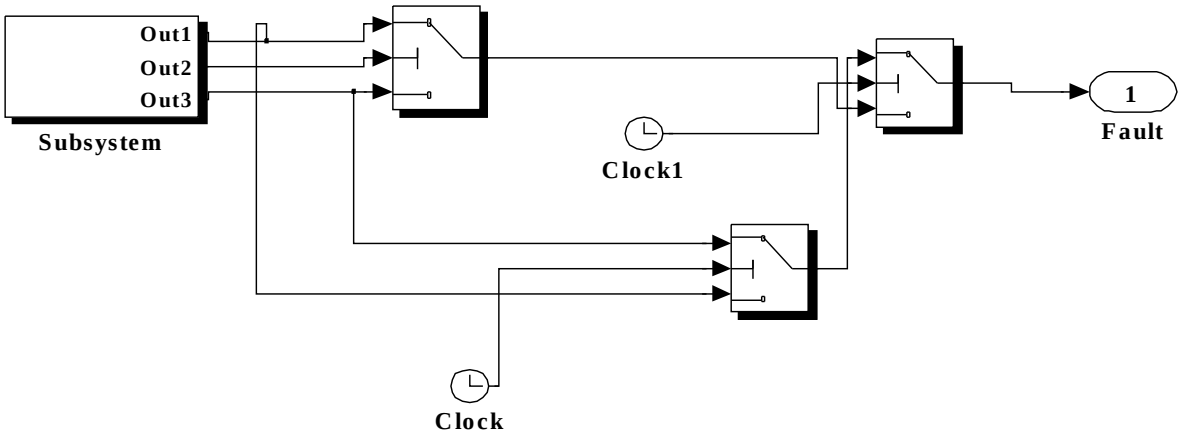

Figure 4.13: The switch configuration of fault

The inner detail of the considered switches in sub-system is shown in Fig. 4.14. This sub system initially gives first operation values to the system via out 3. After a period which is determined by adjusting the clock, the switch changes and new parameter values are collected from out 1.

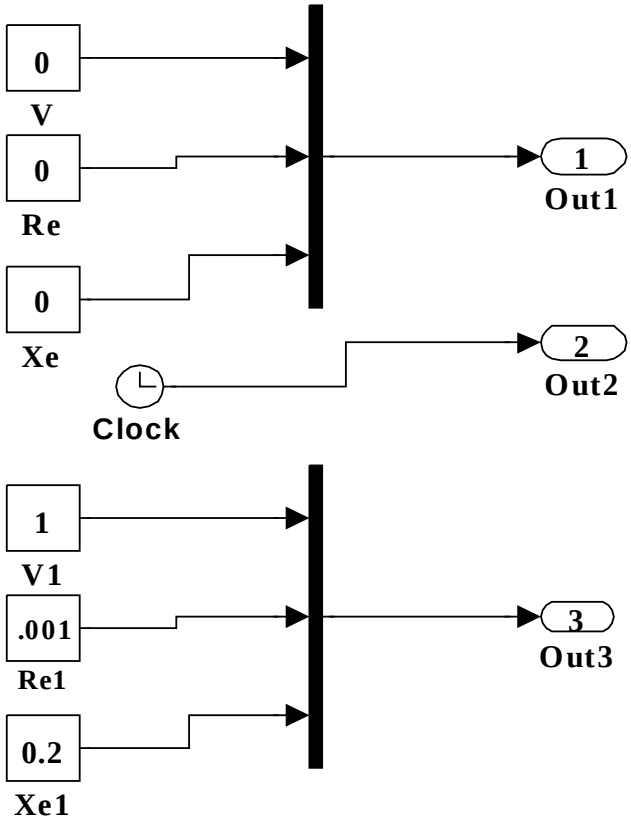

Figure 4.14: Inner detail of the subsystem in fault

CHAPTER 5

RESULTS AND DISCUSSIONS

The development of dynamic models of various components has been discussed in chapter 3. The model equations can be solved by fourth order Runge-Kutta numerical integration method as discussed in chapter 3. The detailed simulation methodology under SIMULINK environment with reference to the system has been discussed in chapter 4. SIMULINK uses a solver based on Runge-Kutta fourth order integration method ode45. The study of the superconducting synchronous generator behaviour has been carried out and some characteristics are compared with comparable capacity conventional generator. The data of superconducting generator are given in appendix.

5.1 PERFORMANCE OF SUPERCONDUCTING GENERATOR

The performance characteristics of superconducting synchronous generator, which are simulated with the developed algorithm as discussed in chapter 3, are shown in Fig. 5.1-5.6. These characteristics are corresponds to direct connection of the superconducting generator driven at synchronous speed, with the input torque 1.11×10^{6} Nm. The initial field voltage is taken as 26kV to produce rated voltage at no load. With the grid connection high initial transients are obtained in all the parameters which decreases gradually. The steady state is attained in 40 sec which are shown in Fig. 5.1-5.6 respectively.

Voltage characteristics are shown for v_{qs} and v_{ds} in Fig. 5.1. v_{qs} starts with 26 kV voltage level where as v_{ds} starts with initial 0 voltage level. Stator current characteristics for superconducting generator are shown in Fig. 5.2.

When generator are connected to grid, current got negative value and after it got positive value. After the transients i_{qs} settles to positive and i_{ds} settles to negative value. These values are decided by rotor angle. Field current characteristic is shown in Fig. 5.3. In starting there are large transients are produced. But during time duration of 40 sec, it got steady state corresponding to rated current.

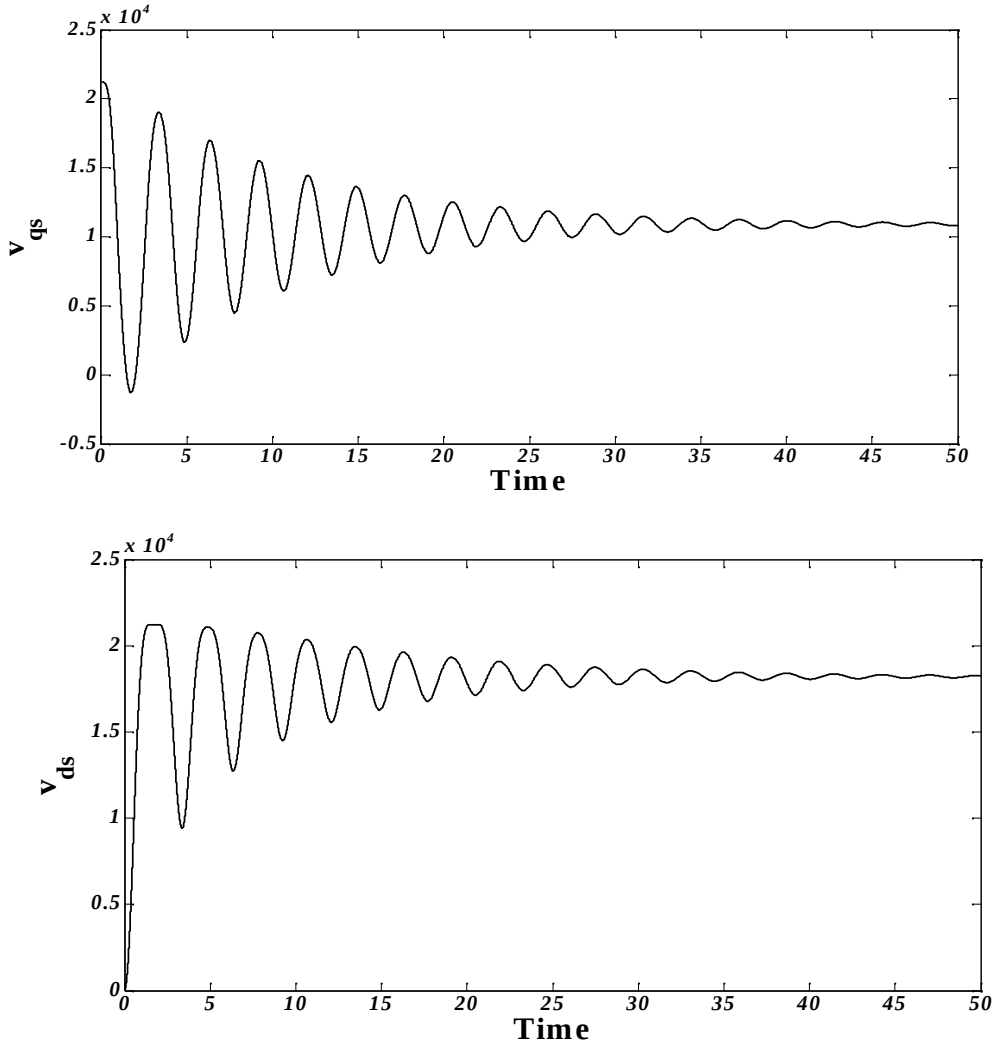

Figure 5.1: Voltage-Time characteristics of superconducting generator

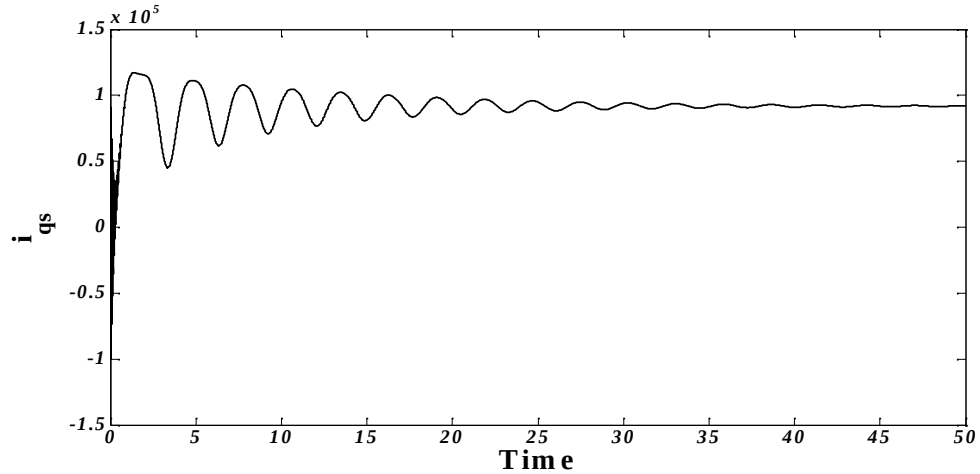

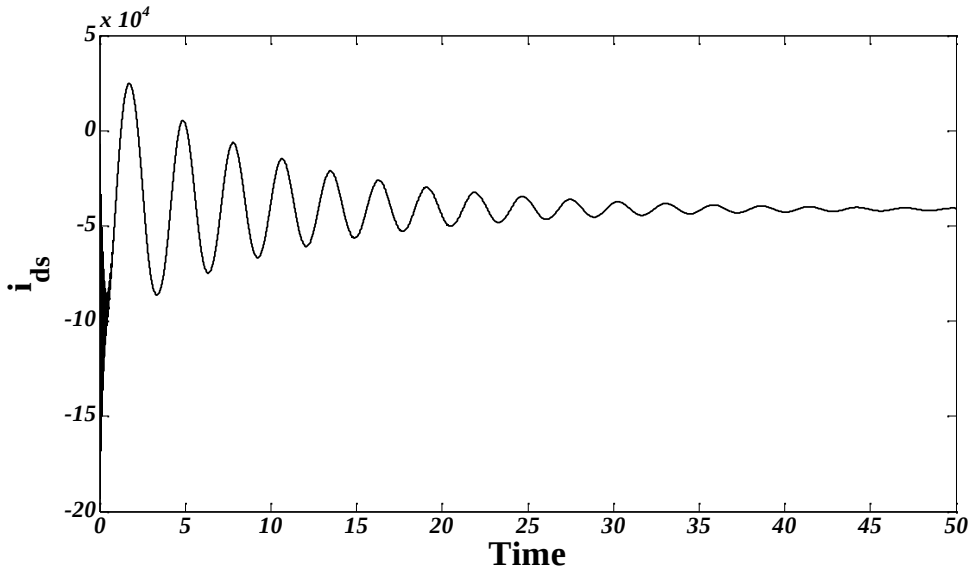

Figure 5.2: Current-Time characteristics of superconducting generator

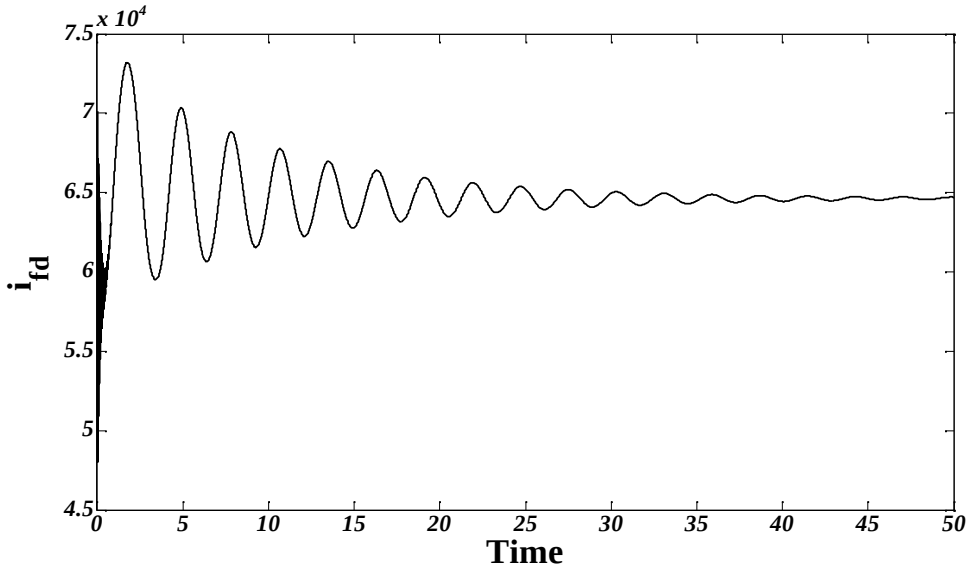

Figure 5.3: Field Current-Time characteristics of superconducting generator

Torque-time characteristics are shown in Fig. 5.4. When generator starts the torque developed negative, and when generator got synchronous speed it got settled down at 1.11×10^{6} Nm.

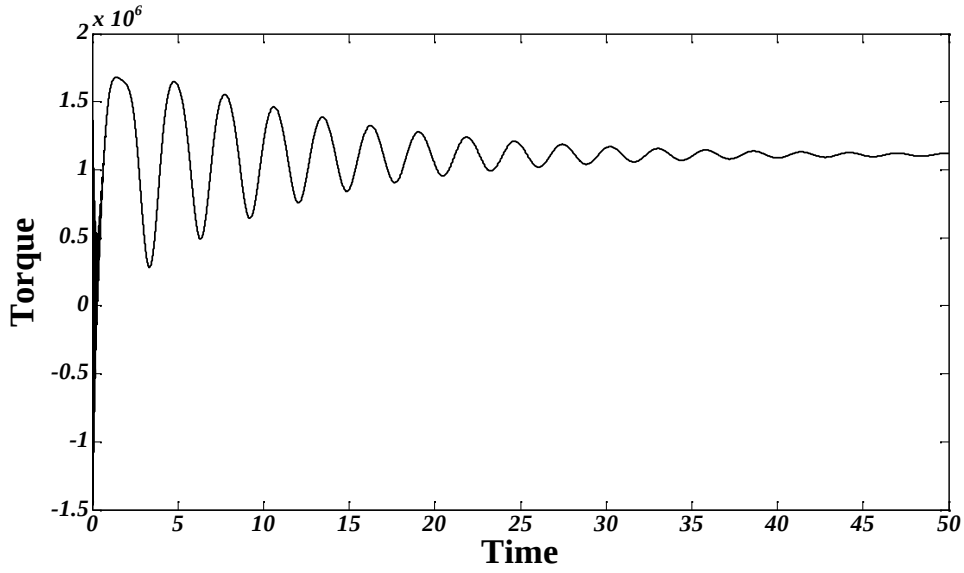

Figure 5.4: Torque-Time characteristics of superconducting generator

Speed characteristic is shown in Fig. 5.5. When generator starts speed increased due to decrease in electric torque and after initial transients it gradually attains constant synchronous speed.

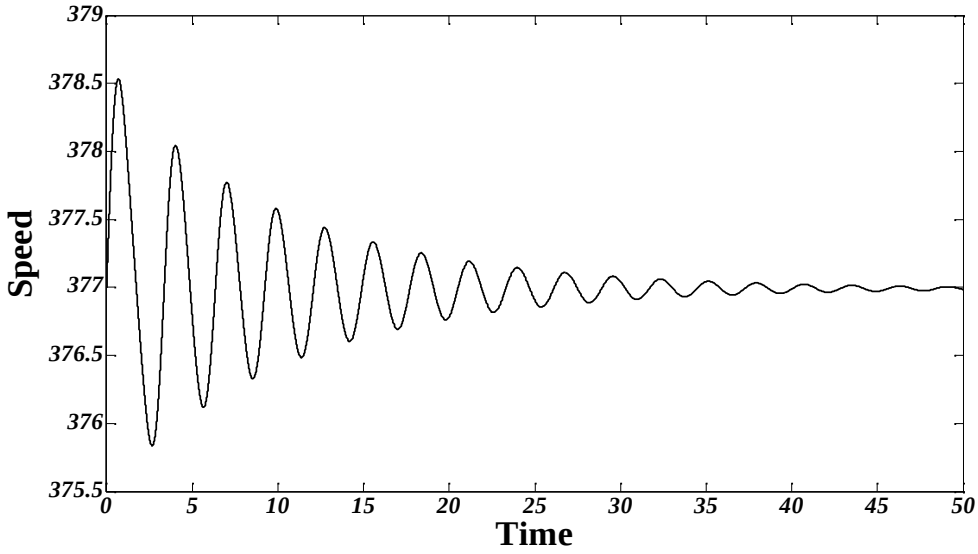

Figure 5.5: Speed-Time characteristics of superconducting generator

Rotor angle (delta) characteristics are shown in Fig. 5.6. Initially when generator starts then delta increase from zero and got large value in starting due to increase in speed and after duration, it attain steady value in around 40 sec.

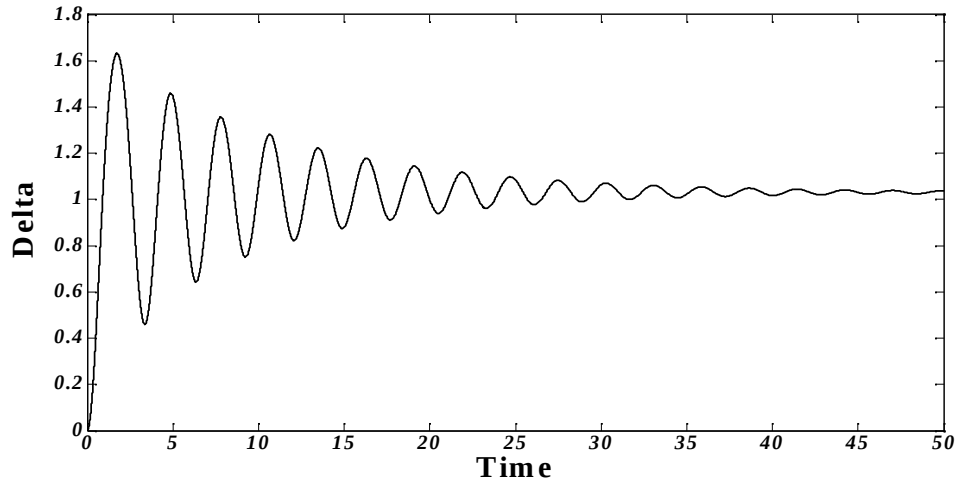

Figure 5.6: Delta-Time characteristics of superconducting generator

The steady state duration is very long and to understand the reason, the performance characteristics are compared with the comparable capacity conventional steam driven generator. The performance of conventional generator is presented in Fig. 5.7 to Fig. 5.12. At the instant of grid connection the similar nature in characteristics are observed. However, the transients decrease and steady state is obtained in small time. This is due to higher inertia and damping due to resistances.

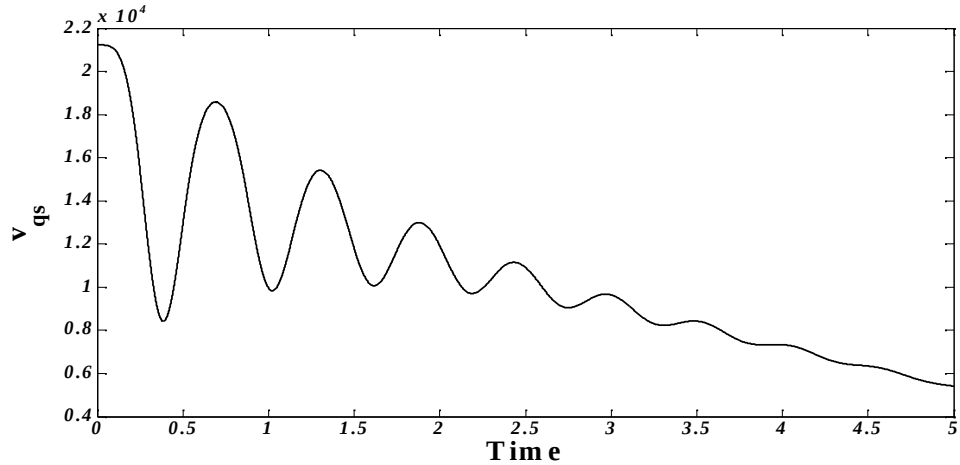

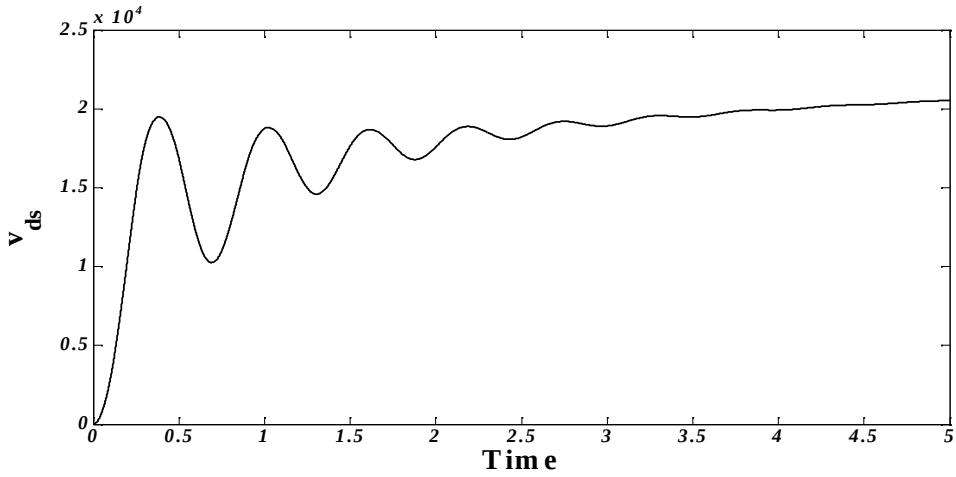

Figure 5.7: Voltage-Time characteristics of conventional generator

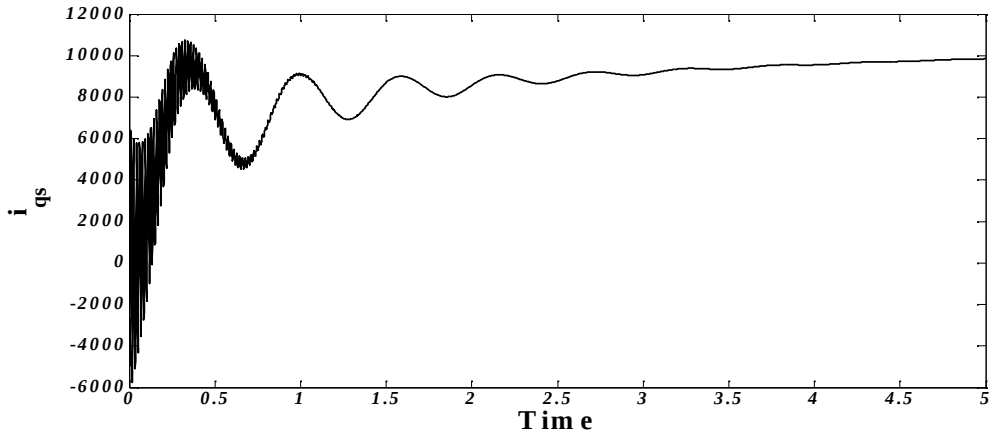

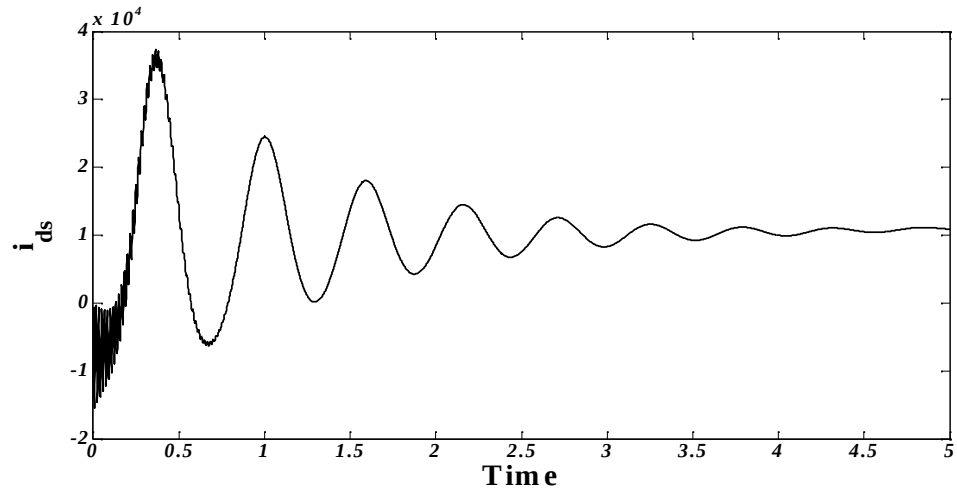

Figure 5.8: Current-Time characteristics of conventional generator

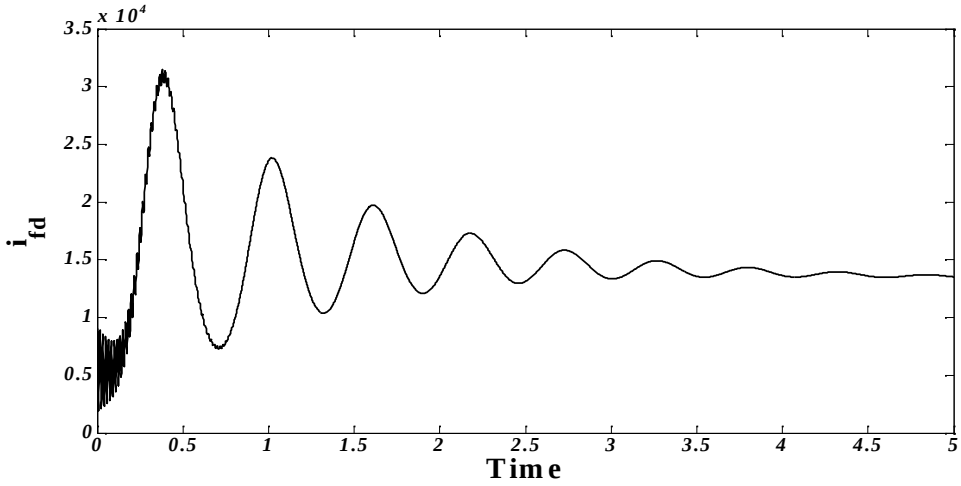

Figure 5.9: Field Current-Time characteristics of superconducting generator

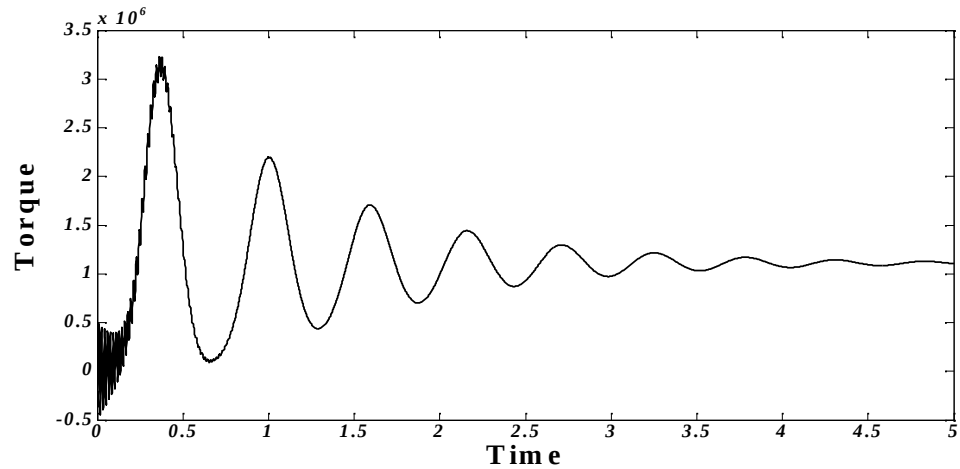

Figure 5.10: Torque-Time characteristics of conventional generator

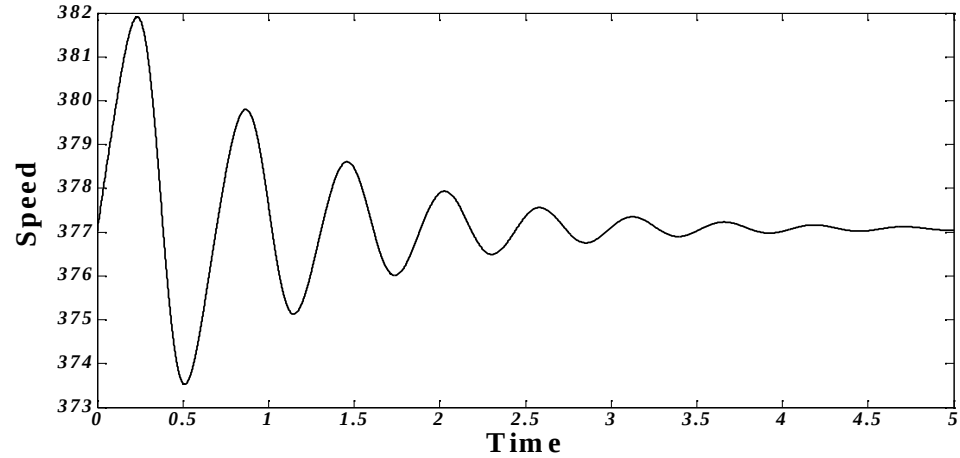

Figure 5.11: Speed-Time characteristics of conventional generator

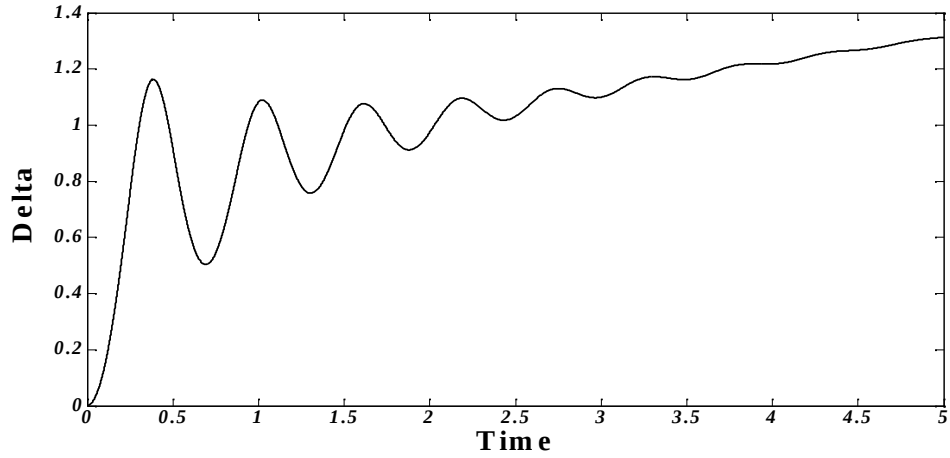

Figure 5.12: Delta-Time characteristics of conventional generator

5.2 PERFORMANCE OF GENERATOR IN SIMULINK

To represent the dynamic system model for simulation of the superconducting generator is constructed by using properly selected sub blocks [33, 35]. The performance characteristics of generator, which are already simulated and has been studied briefly with the help of SIMULINK in chapter 4 are shown in various cases, discussed below for transient analysis, single machine with infinite bus system is shown in Fig. 5.13.

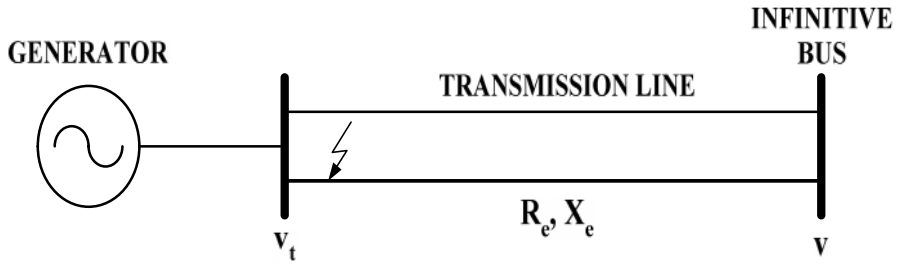

Figure 5.13: Single machine-infinite bus system

Two types of faults are considered at the sending terminal of the parallel transmission lines.

- Three phase short circuit fault.
- Open conductor condition.

All the performance analysis has been done by taking account of these two fault conditions. The three phase short circuit fault has occurred at 0.6 sec and the fault is

continued until 0.78 sec. the fault is cleared by re closing the faulted line at 0.78 sec and then system is returned to the pre-fault configuration. In open conductor fault before the pre-fault condition the faulty line will be out of circuit and the effective reactance of the line will be doubled.

5.2.1 SUPERCONDUCTING GENERATOR WITHOUT STABILIZER.

Terminal voltage-time characteristic without stabilizer is shown in Fig. 5.14. When fault occurred for duration of 0.18 sec, the terminal voltage reduced to zero at 0.6 sec. After fault clearing at 0.78 sec voltage increased and got initial steady state value at 1.2 p.u. Power-time characteristic is shown in Fig. 5.14.

During fault duration power goes approximately zero. But with fault clearing, power increased. In starting it have some transients but after small duration it reduced and attains its initial steady state value at 0.809 p.u.

Rotor angle (delta)-time characteristic is shown in Fig. 5.15. During fault rotor angle (delta) increased to its peak value. With fault clearing it get its initial state at around 39. Delta ω_r characteristic is shown in Fig. 5.16. Change in delta is increased during fault. But in shot duration it got its initial zero value.

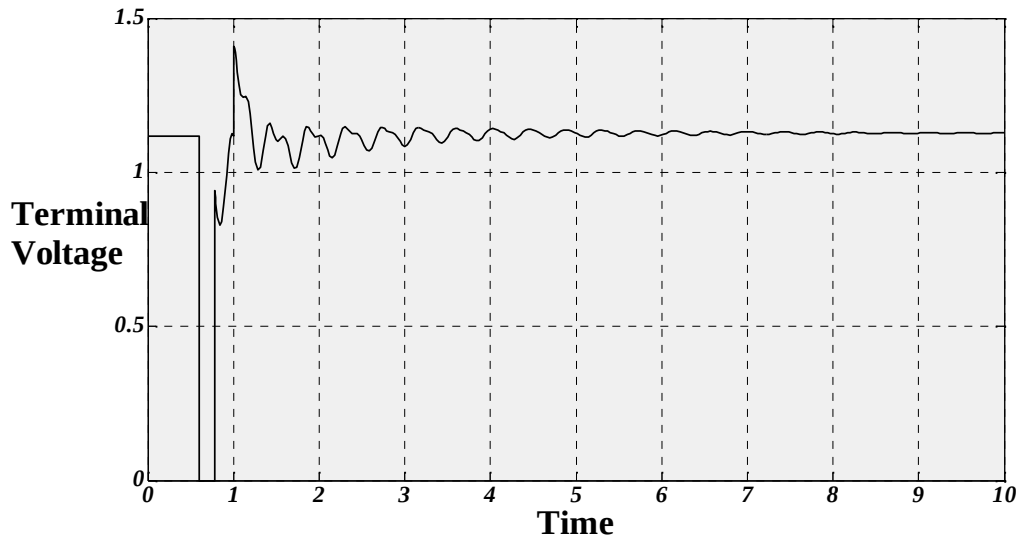

Figure 5.14: Terminal voltage-Time characteristics of superconducting generator

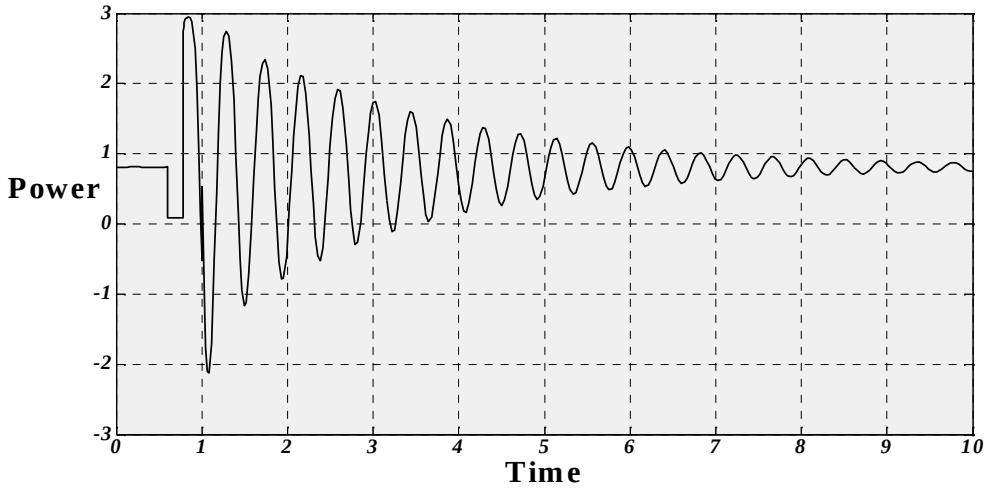

Figure 5.15: Power-Time characteristics of superconducting generator

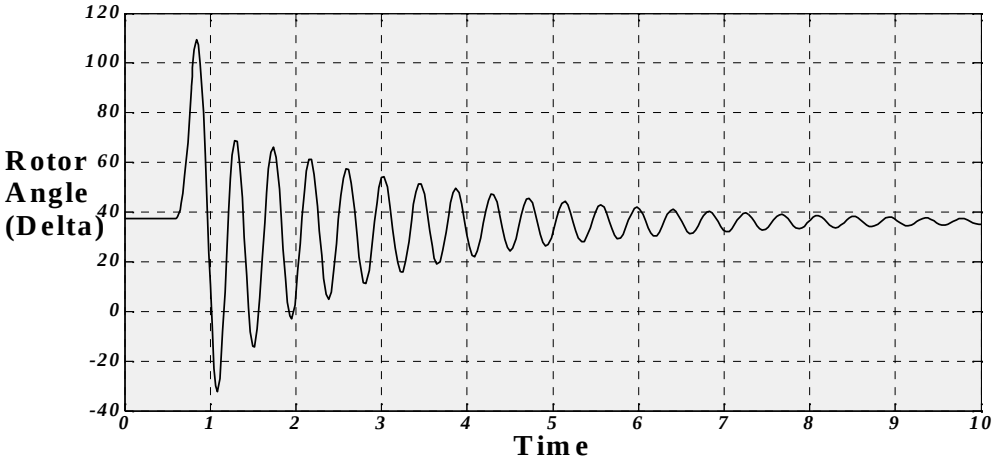

Figure 5.16: Angle (delta)-Time characteristics of superconducting generator

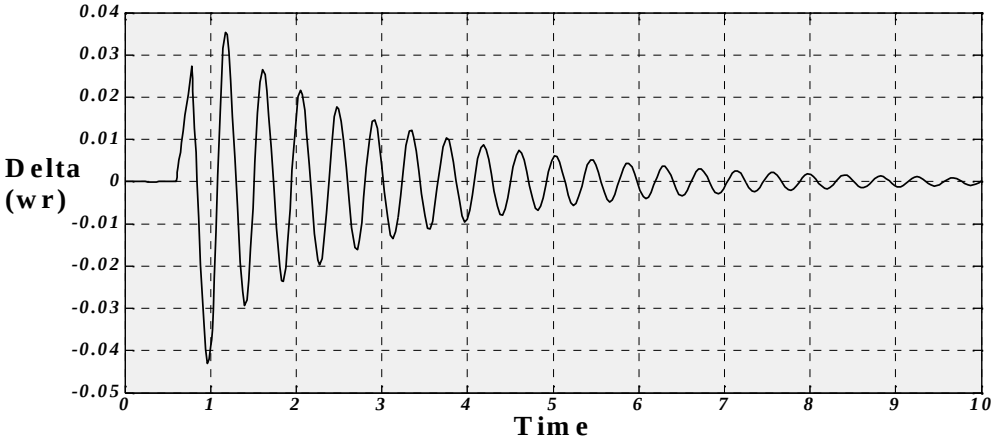

Figure 5.17: Delta (ω_r)-Time characteristics of superconducting generator

5.2.2 COMPARISION OF SUPERCONDUCTING GENERATOR WITH AND WITHOUT STAABILIZER

Terminal voltage-time characteristic for is shown in Fig. 5.18.

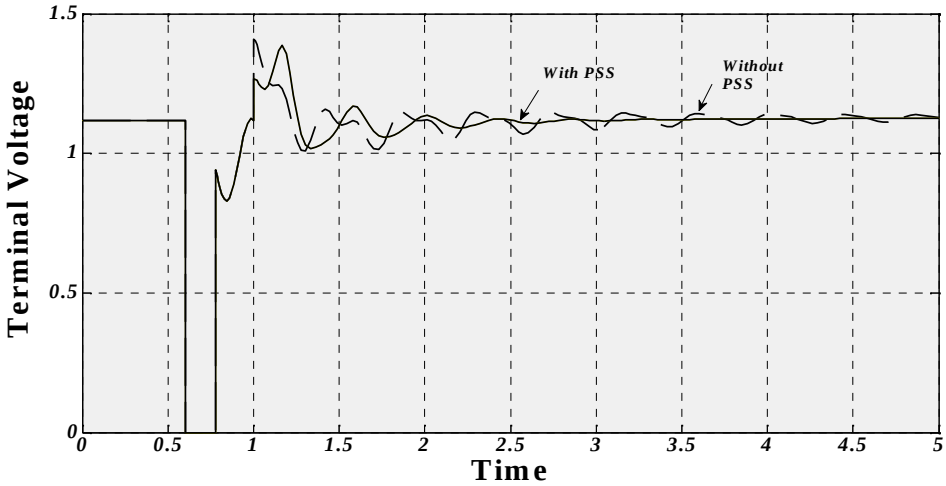

Figure 5.18: Terminal Voltage-Time characteristics of superconducting generator with and without stabilizer.

Here transients are reduced and voltage gets constant value with help of power system stabilizer. Power–time, rotor angle (delta), delta (ω_r) characteristic is shown in Fig. 5.19, 5.20, and 5.21 respectively. Transients are reduced with the help of power system stabilizer and have stable performance because stabilizer is taking auxiliary speed signal to control the excitation.

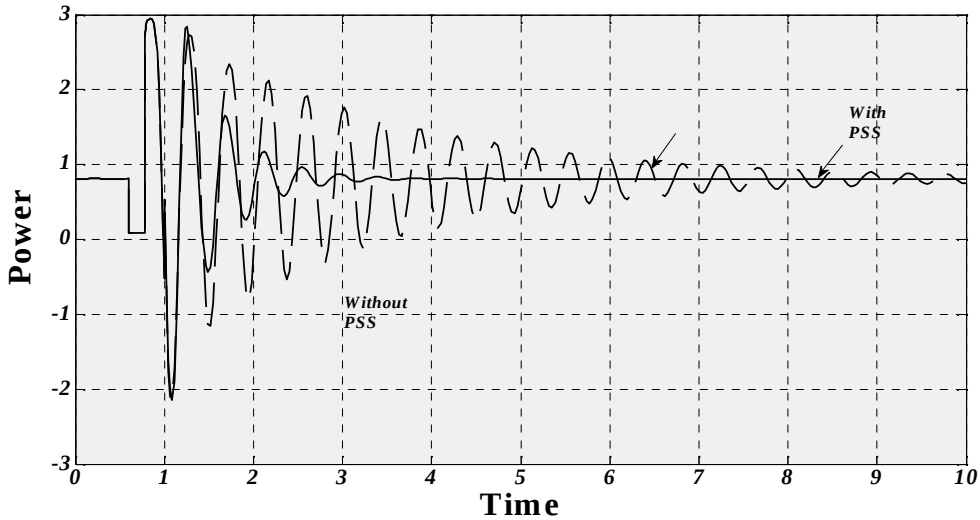

Figure 5.19: Power-Time characteristics of superconducting generator with and without stabilizer.

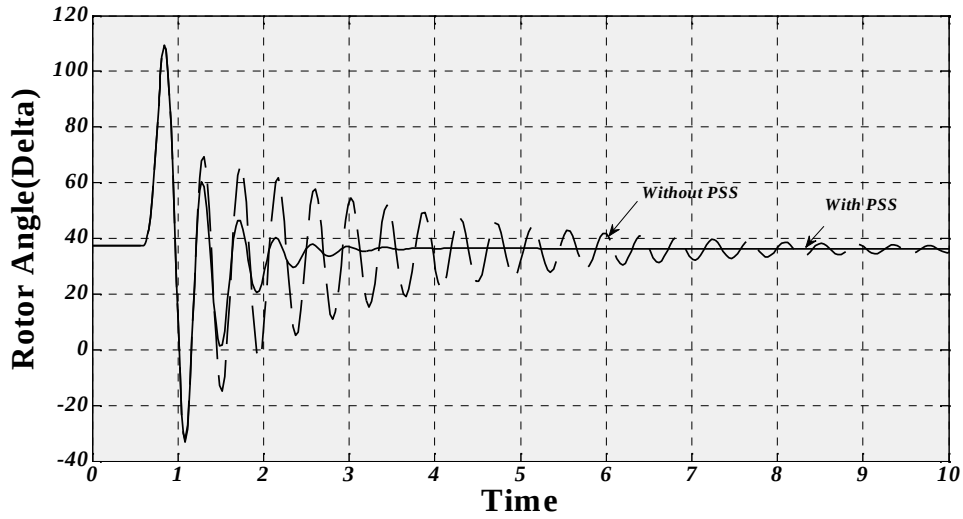

Figure 5.20: Rotor angle(delta)-Time characteristics of superconducting generator with and without stabilizer.

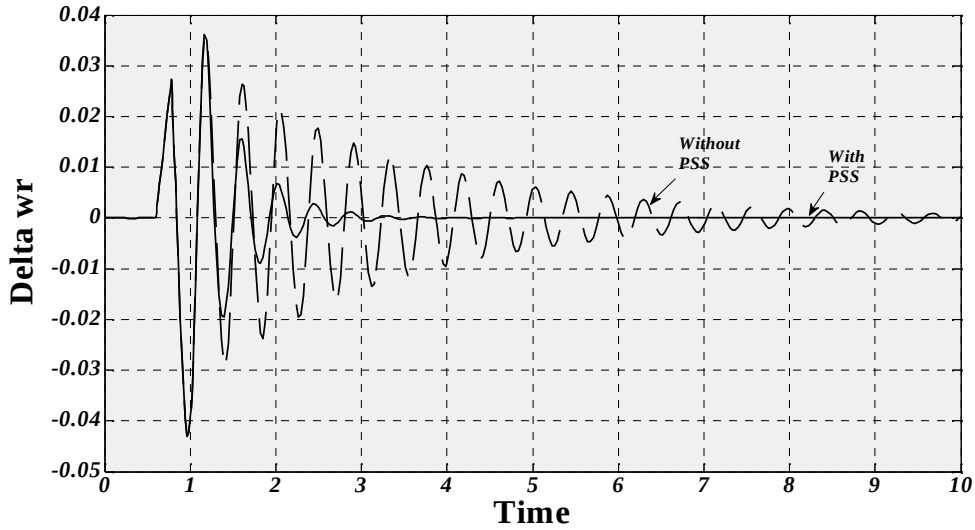

Figure 5.21: Delta (ω_r) -Time characteristics of superconducting generator with and without stabilizer.

5.2.3 COMPARISION OF SUPERCONDUCTING AND CONVENTIONAL GENERATOR WITHOUT STABILIZER

Terminal voltage-time, Power-time, rotor angle, (delta)-time and delta (ω_r)-time characteristics for conventional and superconducting generator are shown in Fig. 5.22, 5.23, 5.24 and 5.25 respectively.

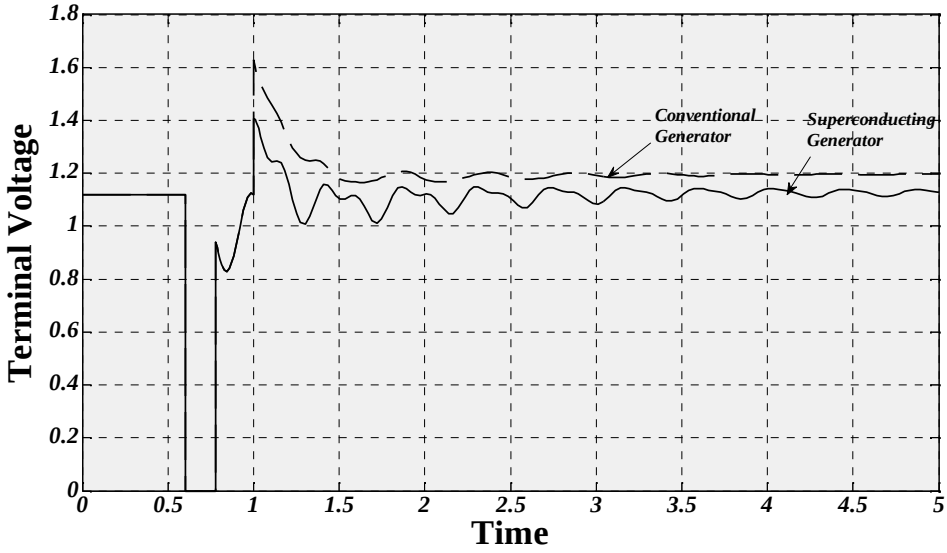

Figure 5.22: Terminal Voltage-Time characteristics of conventional and superconducting generator without stabilizer.

Here fault is occurred for 0.18 sec and after small duration of time both of generators gets their initial steady state values. Conventional generator has less transients and it gets its initial steady state in faster rate as compared to superconducting generator.

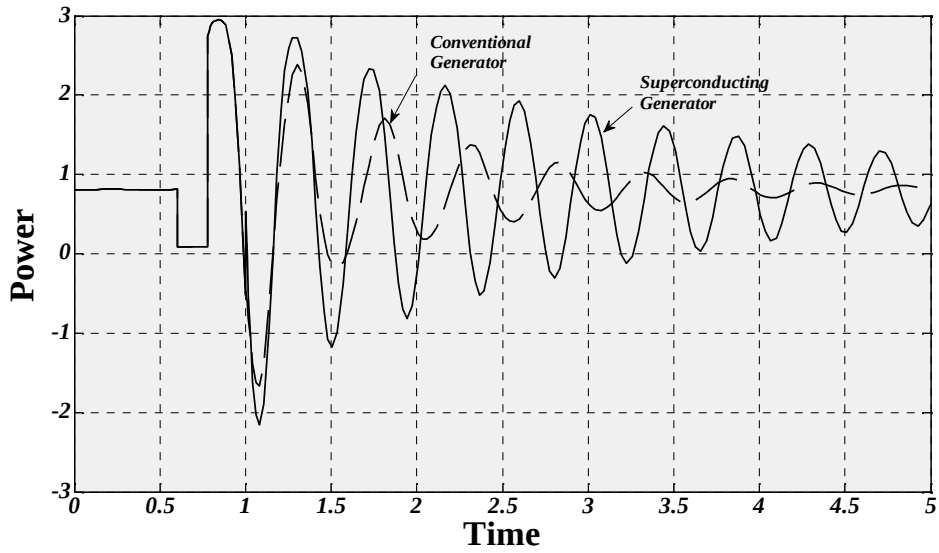

Figure 5.23: Power-Time characteristics of conventional and superconducting generator without stabilizer.

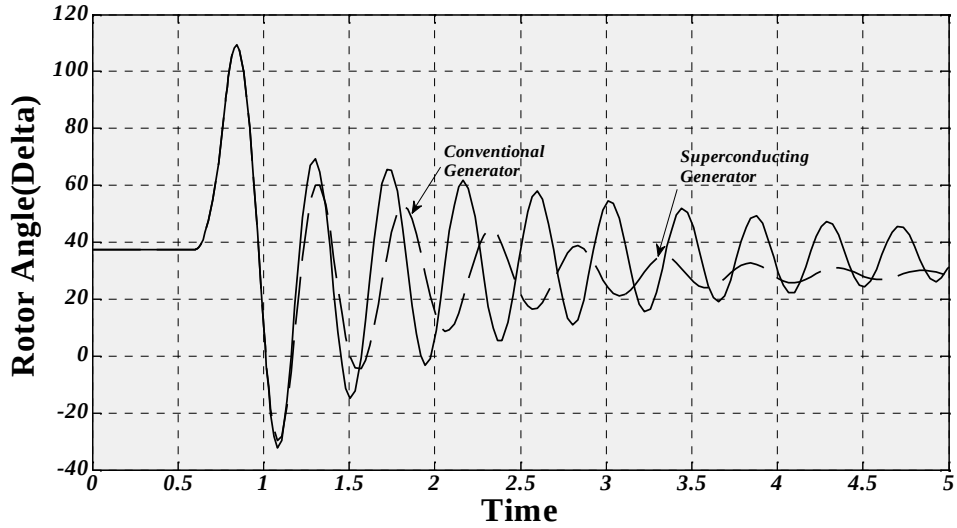

Figure 5.24: Rotor angle (delta)-Time characteristics of conventional and superconducting generator without stabilizer.

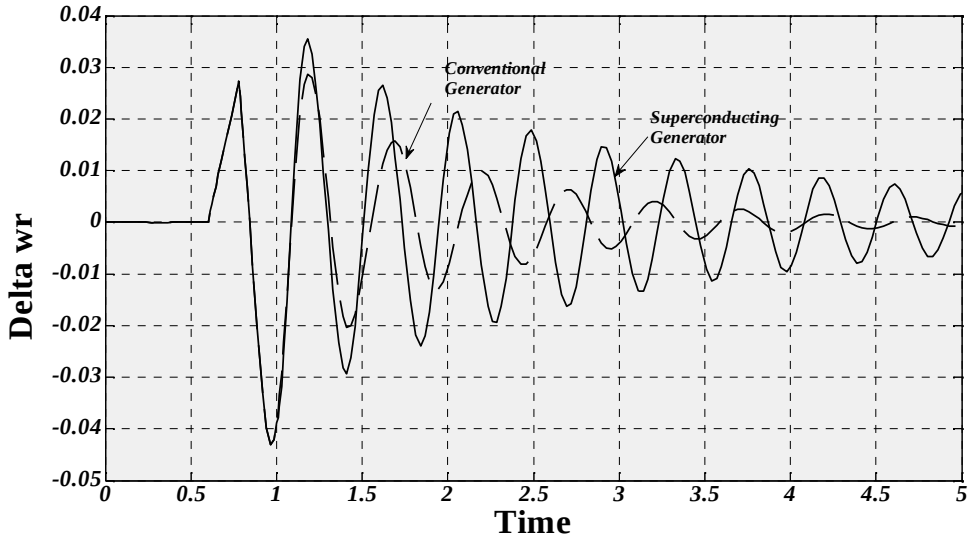

Figure 5.25: Delta (ω_r)-Time characteristics of conventional and superconducting generator without stabilizer.

5.2.4 COMPARISION OF SUPERCONDUCTING AND CONVENTIONAL GENERATOR WITH STABILIZER

Terminal voltage-time, Power-time, rotor angle, (delta)-time and delta (ω_r)-time characteristics for conventional and superconducting generator with power system stabilizer are shown in Fig. 5.26, 5.27, 5.28 and 5.30 respectively.

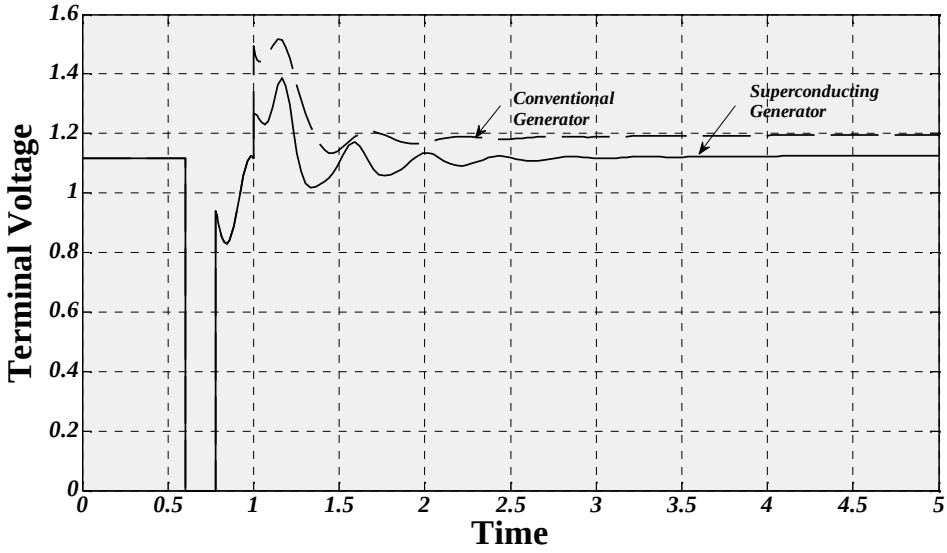

Figure 5.26: Terminal Voltage-Time characteristics of conventional and superconducting generator with stabilizer.

With help of power system stabilizer the transients are reduced. But when short circuit fault occurred for 0.18 sec then due to disturbance transients are developed for small time of duration. Superconducting generator has more transients as compared to the conventional generator and it takes more time to get its steady initial state

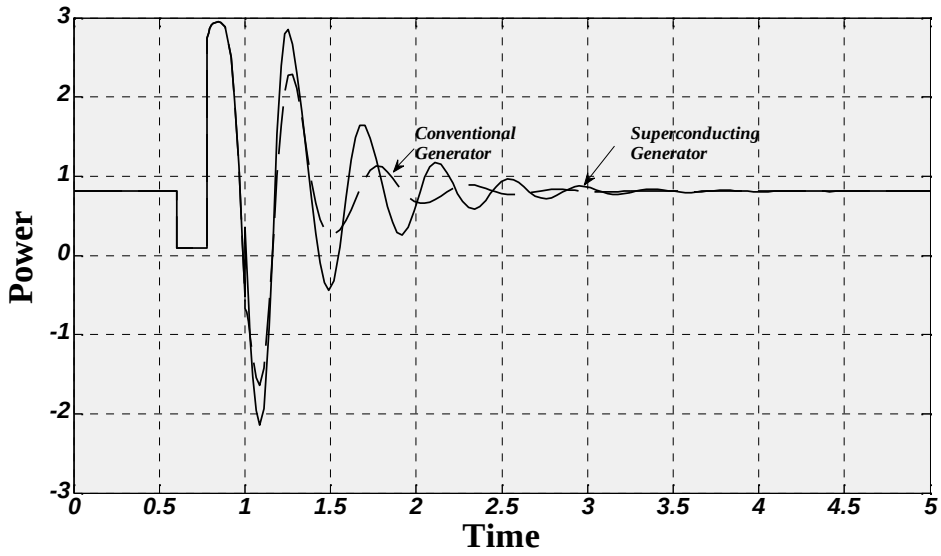

Figure 5.27: Power-Time characteristics of conventional and superconducting generator with stabilizer.

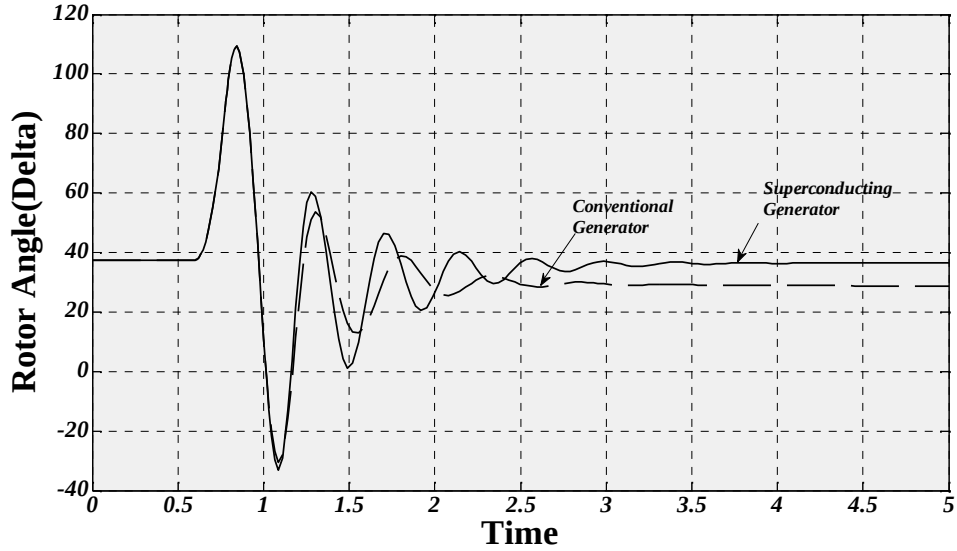

Figure 5.28: Rotor angle (delta)-Time characteristics of conventional and superconducting generator with stabilizer.

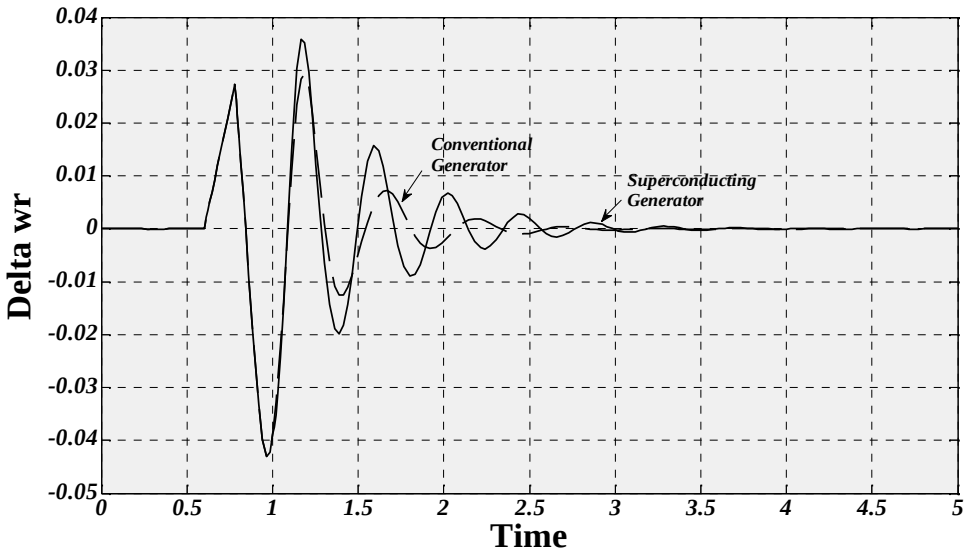

Figure 5.29: Delta (ω_r)-Time characteristics of conventional and superconducting generator with stabilizer.

5.2.5 EFFECT OF SUSTAINED OPEN CONDUCTOR

The model of superconducting generator with infinite bus system is shown in Fig. 5.13. Before the opening of a conductor, it is in the healthy condition and supplying power

with steady state. With the opening of a conductor of parallel transmission line, the effective resistance and reactance offered by the line will be doubled. Due to this, large transients are developed for short duration. But in small time they get its initial steady state. With increase in reactance, power is decreased and generator runs in accelerating mode. It results into increase in speed and rotor angle, as shown in Fig. 5.30, 5.31, 5.32 and 5.33 respectively. The terminal voltage also reduces during transient period, which recovers shortly. These transients are less compared to transients experienced during short circuit fault.

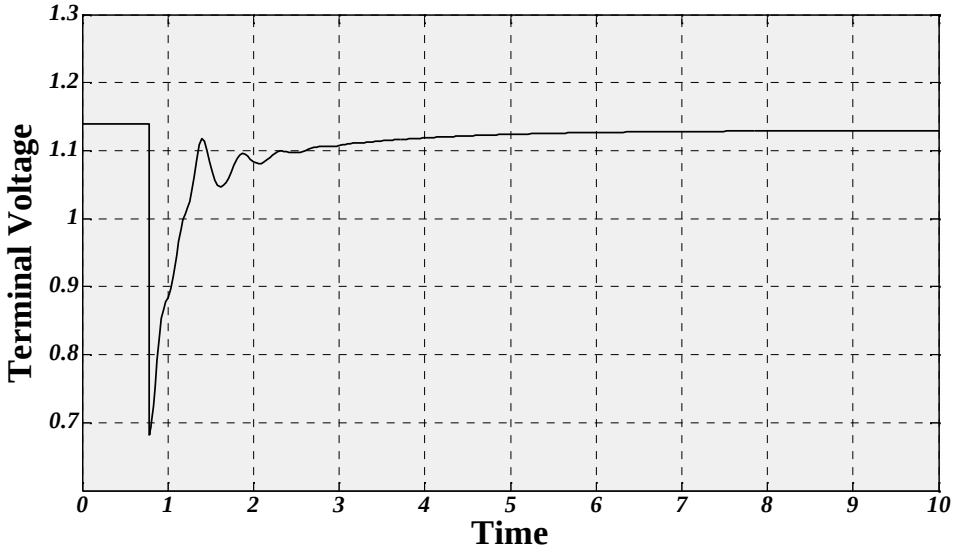

Figure 5.30: Terminal Voltage-Time characteristics.

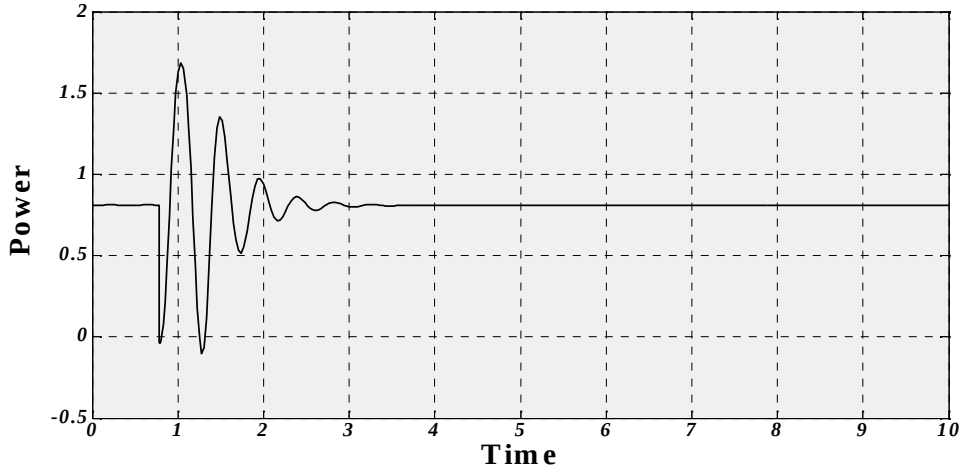

Figure 5.31: Power-Time characteristics

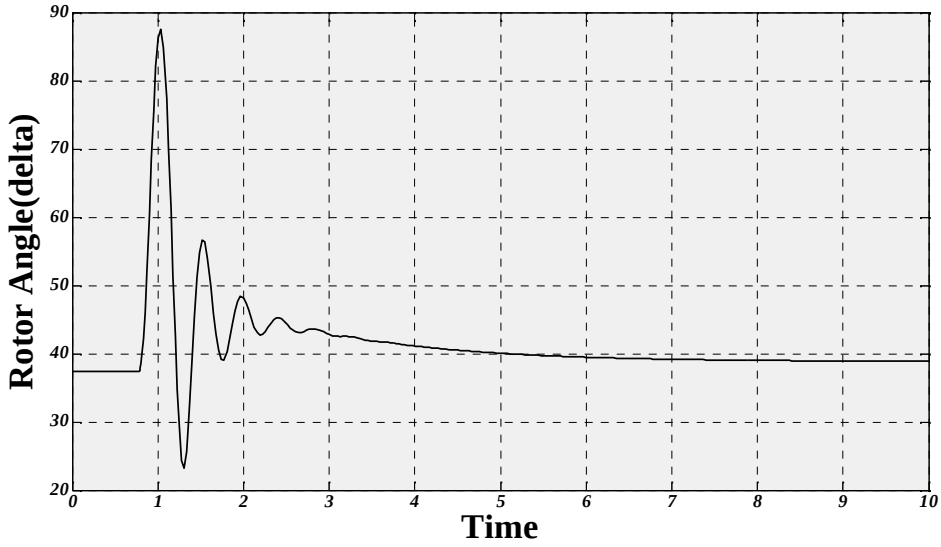

Figure 5.32: Terminal Voltage-Time characteristics

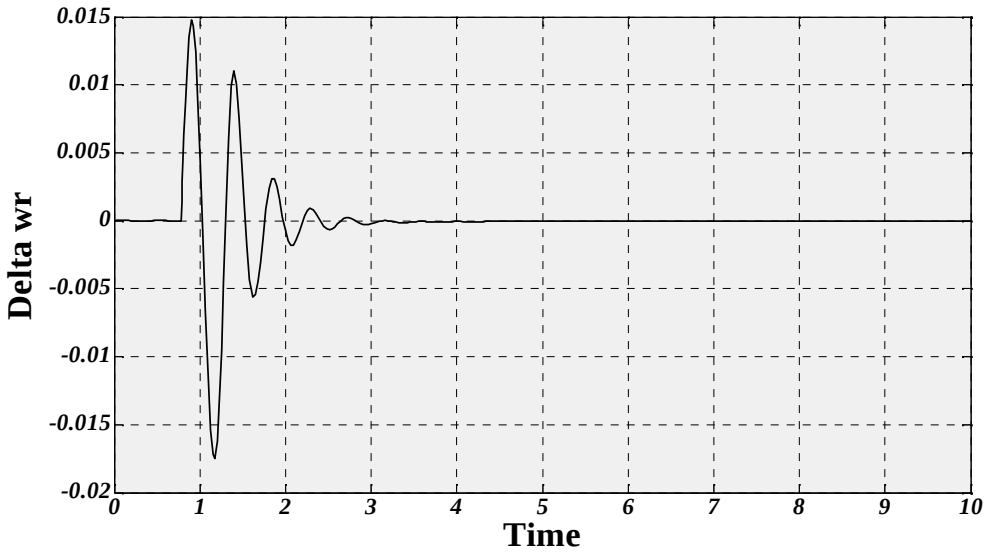

Figure 5.33: Delta (ω_r)-Time characteristics

CHAPTER 6

CONCLUSIONS AND SCOPE OF FUTURE WORK

6.1 CONCLUSIONS

The performance of superconducting generator with exciter, turbine-governor and power system stabilizer, connected to an infinite bus has been analysed by developing the dynamic model. These dynamic models are solved in SIMULINK environment. The performance of generator connected to infinite bus is also studied with Runge-Kutta integration method. The performance is studied for excessive transient cases like grid connection, short circuit fault and opening of the conductor when supplied by a parallel transmission line. The following conclusions are drawn

- During the direct grid connection, the transients are more and are of longer duration because the superconducting machine is characterised by low reactance, low inherent damping and low inertia.
- Power system stabilizer provides the stable performance during fault.
- The transients during sustained opening of a conductor are less then the transients experienced during short circuit fault.
- The conventional generator is showing better performance then superconducting generator because the parameters of exciter, governor, and PSS are corresponding to conventional generator.

6.2 SCOPE OF FUTURE WORK

Having gone through the study of performance analysis of superconducting generator with power system stabilizer for single infinite bus system, the scope of the work has been identified as

- Multi machine system employing superconducting generator, exciter and stabilizer can be investigated.
- Appropriate turbine, governor, exciter, stabilizer models suited for superconducting generator can be explored.

REFERENCES

[1] J. K. Sykulski, K. F.Goddard, and, "Modelling and evaluations of eddy-current loss in high temperature superconducting synchronous generator", IEEE Transactions on Applied Superconductivity, Vol. 2, pp. 370-373, 2006.

[2] J. L. Kirtley, F. J. Edeskuty, "Application of superconductors to motors, generators and transmission lines", IEEE Transactions on Power System, Vol. 77, No. 8, pp. 143-1 154, 1989.

[3] F. Demello, C. Concordia, "Concepts of synchronous machine stability as affected by excitation control", IEEE Transactions on Power Apparatus and System, Vol. 88, No. 4, pp. 316-330, 1969.

[4] A. Godhwani, K. Kim, T. W. Eberly "Commissioning experience with modern digital excitation system", IEEE Transaction on Energy Conversion, Vol. 13, No.2, pp.183-188, 1988.

[5] J. L. Kirtely, "Large system interaction of superconducting generators", IEEE Proceeding on Power System, Vol. 81, No.3, pp.449-461, 1993.

[6] K. Ueda, R. Shiobara, "Measurement and analysis of 70 MW superconducting generator constants", IEEE Transaction on Applied Superconductivity, Vol. 9, No.2, pp. 1193-1196, 1987.

[7] S. S. Ahmed, S. Bashar, "Use of superconducting magnetic energy storage device in a power system to permit delayed tripping", IEEE Proceeding on generation, transmission and Distribution, Vol. 147, No. 5, pp. 269-273, 1995.

[8] R. A. F. Saleh, and H. R. Bolton, "Genetic algorithm-aided design of a fuzzy logic stabilizer for a superconducting generator", IEEE Transactions on Power Systems, Vol. 15, No.4, pp. 1329-1335, 1985.

[9] H. Ying-Yi, W. Wen-Ching, "A new approach using optimization for tunning parameters of power system stabilizers", IEEE Transactions on Energy Conversion, Vol. 14, No. 3, pp. 780-787, 1997.

[10] P. Kundur, M. Klein, "Application of power system stabilizer for enhancement of overall system stability", IEEE Proceeding on Power Engineering, Vol. 9, No. 5, pp. 61-63, 1978.

[11] Z. Lubosny, J. Bialek, “PSS design for a small synchronous generator with static excitation system”, IEEE Proceeding on Power System, Vol. 12, No. 3, pp. 327-332, 2001.

[12] J.J. Dai, F. Shokooh, “Emergency generator startup study of a hydro turbine unit for a nuclear unit for a nuclear generation facility”, IEEE Transaction on Industry Applications, Vol. 40, No. 5, pp. 1191-1120, 2003.

[13] M.A.A.S. Alyan, Y.H.Rahim, “The role of governor control in transient stability of superconducting turbogenerator”, IEEE Transaction on Energy Conversion, Vol. 2, No. 1, pp. 38-47, 1998.

[14] J. Minseok, “Dynamic performance and design of a high temperature superconducting synchronous motor”, IEEE Transaction on Applied Superconductivity, Vol. 9, No. 2, pp.1245-1249, 1986.

[15] J. Michael, “Homopolar generator with high temperature superconductor field windings”, IEEE Transaction on Applied Superconductivity, Vol. 7, No. 2, pp. 513-519, 1989.

[16] J. Evetts, “The characteristics of superconducting material-conflicts and correlations”, IEEE transaction on Magnetics, Vol. 19, No. 3, pp. 1109-1119, 2005.

[17] S.P. Ashworth, B.A. Glowacki, “Connectivity between filaments in BSCCO-2223 multi-filamentary tapes”, IEEE Transaction on Applied Superconductivity, Vol. 7, No. 2, pp. 1662-1666, 2003.

[18] M. Maslouth, F. Bouillaut, “Numerical modelling of superconducting materials using ananistropic”, IEEE Transaction on Magnetics, Vol. 34, No. 5, pp. 3064-3067, 2005.

[19] C. Rose, “A sielectric-free superconducting coaxial cable”, IEEE Transaction on Microwave Theory and Techniques, Vol. 38, No. 2, pp. 166-178, 1999.

[20] R.H. Park, “two reaction theory of synchronous machine-gernalized methods of analysis-Part 1,” AIEE Transactions, Vol. 18, No. 3, pp. 716-723, 2004.

[21] P.C. Krause, “Analysis of Electric Machinery”, McGraw Hill, New York, Vol. 1, 1987.

[22] N. Tanzo, N. Toshihide, “Theoretical and experimental study on characteristics of slow response type superconducting generator for high harmonic armature current”, IEEE Transaction on Applied Superconductivity, Vol. 14, No. 2, pp.892-896, 2004.

[23] P. Kundur, “Power System Stability and Control”, McGraw Hill, New York, Vol. 1, 1994.

[24] A.P. Malozemoff, J.Maguire, S. Kalsi, “ Power application of high temperature superconductors: status and perspectives”, IEEE Transaction on Applied Superconductivity, Vol. 12, No. 1, pp, 778-782, 2000.

[25] J.E. Van, F.M. Brasch, “Analytical investigation of dynamic instability occurring at power station”, IEEE Transaction on Power Apparatus and System, Vol. 99, No. 4, pp. 1386-1396, 1980.

[26] J.Machowski, J.W. Bialek, “Excitation control system for use with synchronous generator”, IEEE Proceeding on Generation, Transmission and Distribution, Vol. 145, No. 5, pp. 537-547, 1998.

[27] D. Kosterev, “Hydro turbine-governor model validation in pacific northwest”, IEEE Transaction on Power System, Vol.19, No. 2, pp. 1144-1150, 2004.

[28] M.C. Jackson, S.D. Umans, R.D. Dunlop, “Turbine-generator shaft torque and fatigue: part-I – simulation methods and fatigue analysis”, IEEE Transaction on Power Apparatus and system, Vol. 98, No. 6, pp. 2299-2208, 1979.

[29] P.B. Roemer, J.A. Mallick, “Three dimensional transient analysis of superconducting generator”, IEEE Transaction on Power Apparatus and System, Vol. 98, No. 6, pp. 2055-2065, 1979.

[30] A. Murdoch, S. Venkataraman, “Integral of accelerating power type PSS part1-theory, design and tuning methodology”, IEEE Transation on Energy conversion, Vol. 14, No. 4, pp. 1658- 1664, 1994.

[31] R.M. Mathur, J.Jing, G.L.Rogers, “Modelling of generator and their control in power system simulations using singular perturbations”, IEEE Transaction on Power System, Vol. 13, No. 1, pp. 109-115, 1998.

[32] B. Miljenko, K. Igor, “Nonlinear digital simulation model of hydro electrical power unit with Kaplan turbine”, IEEE Transaction on Energy Conversion, Vol. 21, No. 1, pp.235-242, 2006.

[33] A. Demiroren, H.L. Zeynlgil, “Modelling and simulation of synchronous machine transient analysis using SIMULINK”, International Journal of Electrical Engineering Education, Vol. 39, No. 4, pp.337-347, 2002.

[34] C.W. Taylor, “Power System Voltage Stability”, McGraw Hill, New York, Vol. 2, 1994.

[35] S.M. Osheba, M.A.A.S. Alyan, “Comparision of transient performance of superconducting and conventional generator in multi machine system”, IEEE Proceedings, Vol. 135, No. 5, pp. 388-395, 1988.

APPENDIX

Table: Parameters of conventional and superconducting generator [5]

Parameters	Conventional Generator	Superconducting Generator
Rated MVA	907	907
Voltage	26	26
Pole	2	2
F	60	60
J	0.04002×10^{6}	0.0136×10^{6}
R_s	0.0038	0.0019
R_{kq1}	0.3713	2.032×10^{-4}
R_{kq2}	0.3713	2.03×10^{-4}
R_{fd}	0.0011	4.4988×10^{-7}
R_{kd}	5.408×10^{-3}	2.093×10^{-4}
X_d	2.22	0.197
X_q	2.09	0.197
X_{lkq1}	0.196	0.1193
X_{lkq2}	0.196	0.1193
X_{lkd}	0.2095	0.122
X_{lfd}	0.2158	0.2522
P_o	0.8	0.8
Q_o	0.496	0.496
V_o	1	1
R_a	0.0038	0.0019

R_e	0.01	0.01
X_d	2.22	0.297
X_q	2.09	0.297
X'_d	0.245	0.209
X_e	0.2	0.2
T'_{do}	5.9	1487
T'_{qo}	0.075	1.557
K_e	400	400
T_e	0.05	0.05
K_f	0.025	0.025
T_{fe}	0.025	0.025
D	0	0
M	4.74	4.74
ω_0	1	1
T_{rh}	8	8
T_{ch}	0.05	0.054
T_{sr}	0.1	0.1
K_g	3.5	3.5
T_{sm}	0.2	0.2
ω_r	1	1